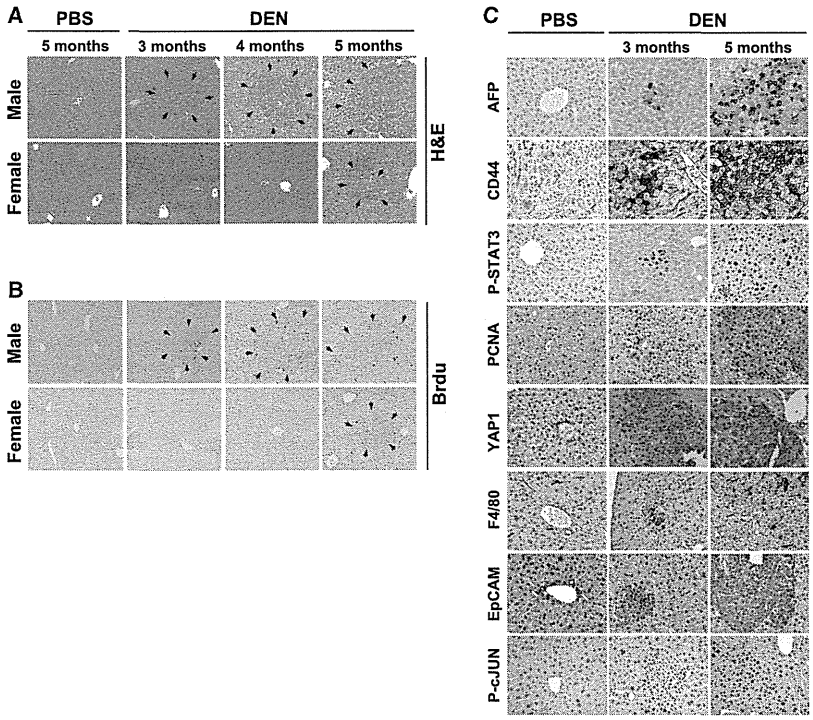

Figure 5. HcPC-Containing Aggregates May Originate from Liver Premalignant Lesions

(A and B) Male and female mice were injected with PBS or DEN at 15 days. At the indicated time points, BrdU was administrated, and livers were collected 2 hr later and stained with H&E (A) or a BrdU-specific antibody (B). Arrows indicate borders of FAH (magnification: 200×).

(C) Sections of male livers treated as above were subjected to IHC with the indicated antibodies (400×).

factors that control IL-6 expression and found that LIN28A and B were significantly upregulated in HcPCs and HCC (Figures 6D and 6E). LIN28-expressing cells were also detected within FAH (Figure 6F). As reported (Iliopoulos et al., 2009), knockdown of LIN28B in cultured HcPC or HCC cell lines decreased IL-6 expression (Figure 6G). LIN28 exerts its effects through downregulation of the microRNA (miRNA) Let-7 (Iliopoulos et al., 2009). Accordingly, miRNA array analysis of aggregated and nonaggregated hepatocytes from DEN-treated mice indicated that the amount of Let-7, along with other miRNAs that also inhibit IL-6 expression (miR194 and miR872), was lower in aggregated cells than in nonaggregated cells (Table S2).

To determine whether autocrine IL-6 production is needed for HCC growth, we silenced IL-6 expression with small hairpin RNA (shRNA) in dih10 HCC cells (He et al., 2010). This resulted in nearly a 75% decrease in IL-6 mRNA (Figure 7A) but had little effect on cell growth in the presence of growth factors, including EGF and insulin (Figure S6A). IL-6 mRNA silencing, however, diminished the ability of dih10 cells to form s.c. tumors (Figures S6B and S6C) and inhibited their ability to form HCCs and proliferate after transplantation into MUP-uPA mice (Figures 7B and S6D). To investigate the importance of autocrine IL-6 production at an earlier step, we isolated HcPC from DEN-treated WT and *Il6*$^{-/-}$ mice. Although IL-6 ablation attenuates HCC induction (Naugler et al., 2007), we still could isolate collagenase-resistant aggregates from livers of DEN-injected *Il6*$^{-/-}$ mice. Notably, IL-6 ablation did not reduce the proportion of CD44^{+} cells in the aggregates (Figures S7A and S7B). We introduced an identical number of WT and *Il6*$^{-/-}$ aggregated hepatocytes into MUP-uPA mice and scored HCC development 5 months later. The IL-6 deficiency resulted in a 2.5-fold decrease in tumorigenic potential (Figure 7C), suggesting that autocrine IL-6 contributes to HcPC to HCC progression. To confirm this point, we dispersed freshly isolated DEN-induced aggregates and transduced them with bicistronic lentiviruses encoding either scrambled or IL-6-specific shRNAs and a GFP marker. After a few days in culture, the transduced cells were introduced into MUP-uPA mice that were examined for HCC development 6 months later. Silencing of IL-6 reduced HCC generation (Figure 7D) and inhibited formation of GFP^{+} colonies within the MUP-uPA liver (Figure 7E). We also ablated IL-6 expression in mouse hepatocytes and found that this led to a marked reduction in DEN-induced tumorigenesis (Figure 7F). Thus, autocrine IL-6 production by DEN-initiated HcPC is important for HCC development. To investigate whether autocrine IL-6 signaling also occurs in human premalignant lesions, we examined needle biopsies of normal liver tissue and HCV-infected livers with dysplastic lesions. We found that 16% of all (n = 25) dysplastic lesions exhibited coexpression of LIN28 and IL-6 and contained activated STAT3 (Figure 7G). These markers were hardly detected in normal liver or nontumor portion of HCV-infected livers.

DISCUSSION

The isolation and characterization of cells that can give rise to HCC only after transplantation into an appropriate host liver undergoing chronic injury demonstrates that cancer arises from progenitor cells that are yet to become fully malignant. Importantly, unlike fully malignant HCC cells, the HcPCs we isolated cannot form s.c. tumors or even liver tumors when introduced into a nondamaged liver. Liver damage induced by uPA expression or CCl_4 treatment provides HcPCs with the proper cytokine and growth factor milieu needed for their proliferation. Although HcPCs produce IL-6, they may also depend on other cytokines such as TNF, which is produced by macrophages that are recruited to the damaged liver. In addition, uPA expression and CCl_4 treatment may enhance HcPC growth and progression through their fibrogenic effect on hepatic stellate cells. Although HCC and other cancers have been suspected to arise from

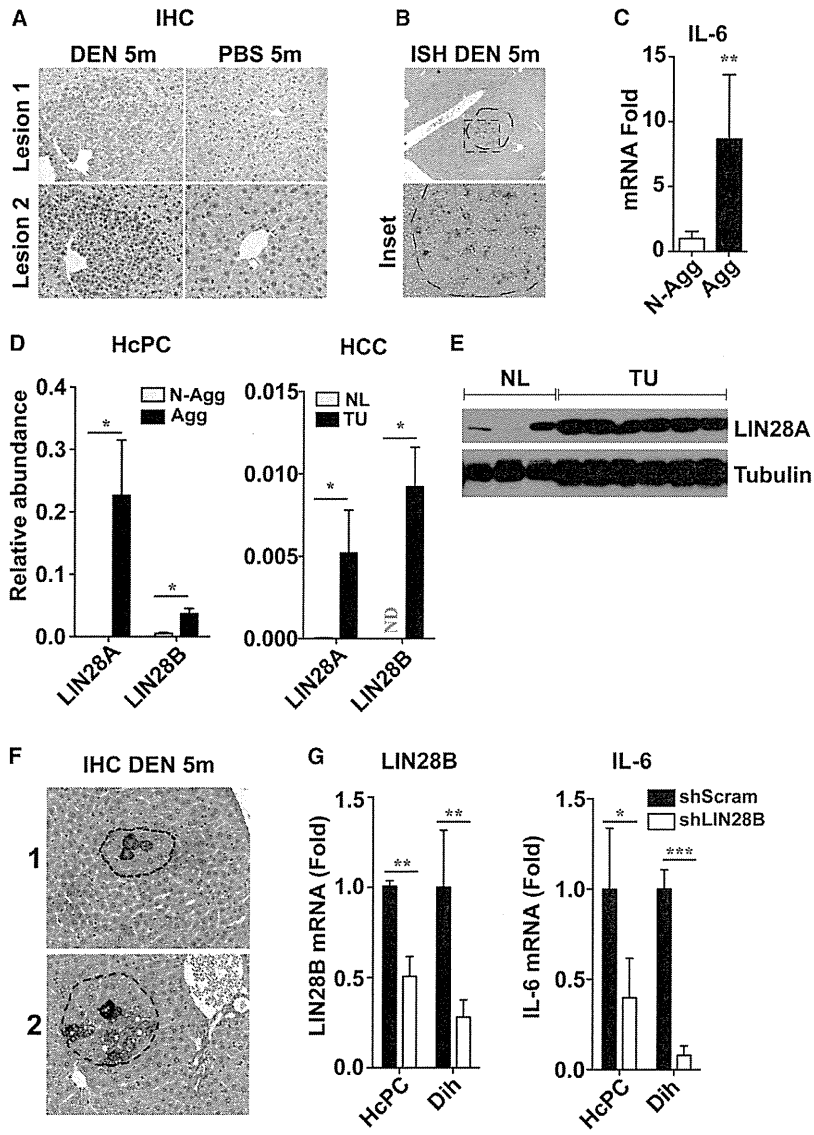

Figure 6. Liver Premalignant Lesions and HcPCs Exhibit Elevated IL-6 and LIN28 Expression

(A and B) Livers of 5-month-old DEN injected mice were analyzed for IL-6 expression by IHC (magnification: 400×) (A) and ISH (magnification: 100×, top; 400×, bottom) (B).

(C and D) Quantification of IL-6 (C) and LIN28 (D) mRNA in aggregated versus nonaggregated hepatocytes from 5-month-old DEN-treated livers and in normal versus tumor-bearing livers (n = 6; ± SEM) (ND, not detected).

(E) Immunoblot analyses of LIN28A in normal (NL) and tumor-bearing (TU) livers.

(F) DEN-treated livers were subjected to IHC with a LIN28A antibody. Broken lines indicate borders of FAH (400×).

(G) LIN28B was silenced with shRNA in HCC (dih) cells and cultured HcPCs, and LIN28B and IL-6 mRNAs were quantitated by qRT-PCR (n = 3; ± SEM).

See also Figure S5 and Table S2.

premalignant/dysplastic lesions (Hruban et al., 2007; Hytiroglou et al., 2007), a direct demonstration that such lesions progress into malignant tumors has been lacking. Based on expression of common markers—EpCAM, CD44, AFP, activated STAT3, and IL-6—that are not expressed in normal hepatocytes, we postulate that HcPCs originate from FAH or dysplastic foci, which are first observed in male mice within 3 months of DEN exposure. Indeed, the cells that are contained within the FAH are smaller than the surrounding parenchyma and are similar in size to isolated HcPCs. Importantly, FAH or premalignant dysplastic foci are not unique to DEN-treated rodents (Bannasch, 1984; Rabes, 1983), and similar lesions were detected in human cirrhotic livers (Hytiroglou et al., 2007; Seki et al., 2000; Takayama et al., 1990) in which the rate of HCC progression is 3%–5% per year (El-Serag, 2011). We found that human dysplastic lesions and mouse FAH and HcPC exhibit autocrine IL-6 signaling. HcPC are not unique to DEN-treated mice, and similar cells were isolated from *Tak1*$^{\Delta hep}$ mice in which HCC development resembles cirrhosis-associated human HCC (Inokuchi et al., 2010).

HcPC Origin and Relationship to Liver and HCC Stem Cells

Transcriptomic analysis indicates that DEN-induced HcPCs are related to both normal hepatobiliary bipotential stem cells/oval cells and HCC cells. Although HcPCs are not fully transformed, they express several markers—CD44, EpCAM, AFP, SOX9, OV6, and CK19—found to be expressed by HCC stem cells and oval cells (Guo et al., 2012; Mikhail and He, 2011; Terris et al., 2010; Yamashita et al., 2008; Zhu et al., 2010). However, unlike oval cells, which do not express albumin or AFP and do not give rise to liver tumors upon transplantation into MUP-uPA mice, HcPCs give rise to HCC after intrasplenic transplantation. Yet, unlike dih10 HCC cells, which express high levels of the HCC stem cell markers AFP, CD44, and EpCAM, HcPCs do not form s.c. tumors.

At this point, it is not clear whether HcPCs arise from oval cells or from dedifferentiated hepatocytes. Given that DEN is metabolically activated by Cyp2E1 that is expressed only in fully differentiated zone 3 hepatocytes (Tsutsumi et al., 1989) and that *Cyp2E1*$^{-/-}$ mice are refractory to DEN (Kang et al., 2007), DEN-induced HcPC are most likely derived from dedifferentiated hepatocytes. Consistent with this hypothesis, DEN-induced FAH and proliferating cells were found in zone 3 and not near bile ducts or the canals of Hering, sites at which oval cells reside

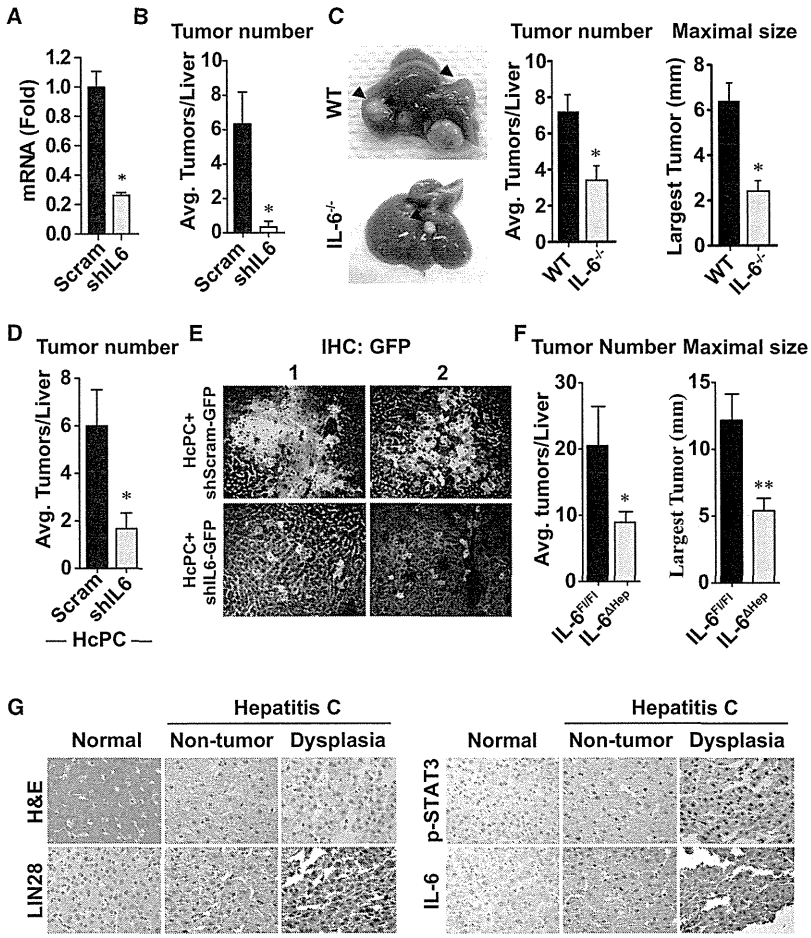

Figure 7. HCC Growth Depends on Autocrine IL-6 Production

(A) HCC cells (dih10) were transduced with lentiviruses containing scrambled or IL-6-specific shRNA. IL-6 mRNA was analyzed by qRT-PCR.

(B) Dih10 cells (1.2×10^5) transduced as above were i.s. injected into MUP-uPA mice that were analyzed 6 months later for HCC development (n = 3; ± SEM).

(C) HcPCs from WT and *Il6*$^{-/-}$ mice were injected (1×10^4 cells/mice) into MUP-uPA mice and analyzed 5 months later for HCC development (n = 5; ± SEM).

(D) HcPCs isolated from DEN-treated WT mice were transduced with shRNA against IL-6 or scrambled shRNA, cultured for 3 to 4 days, i.s. transplanted (1×10^4 cells/mice) into MUP-uPA mice, and analyzed 6 months later (n = 3; ± SEM).

(E) Livers of MUP-uPA mice from (D) were immunostained with GFP antibody 6 months after transplantation (200×). The bicistronic lentivirus in this experiment expresses GFP along with control or IL-6 shRNA, allowing tracking of the infected cells.

(F) DEN-treated *Il6*$^{\Delta hep}$ and *Il6*$^{F/F}$ mice were sacrificed after 9 months to evaluate tumor multiplicity and size (n = 6–10, ± SEM).

(G) IHC analysis of autocrine IL-6 signaling in human premalignant lesions in HCV-infected livers. Expression of LIN28, p-STAT3, and IL-6 was analyzed in 25 needle biopsies of dysplastic nodules, and representative positive specimens (n = 4) are shown. The dysplastic nodules and paired nontumor tissue were obtained from the same HCV-infected patient (n = 25). Nontumor tissue of metastatic liver cancer was used as normal control.

See also Figures S6 and S7.

(Duncan et al., 2009). Notably, GO analysis revealed that many of the genes whose expression is downregulated in HcPC-containing aggregates are involved in xenobiotic and organic acid metabolism, characteristics of differentiated hepatocytes. The same types of genes are also downregulated in HCC. However, final identification of the origin of HcPC will be provided by ongoing lineage-tracing experiments.

The Significance of Autocrine IL-6 Expression

Elevated IL-6 was detected in at least 40% of human HCCs, where it is expressed by the cancer cells (Soresi et al., 2006). More recent studies have confirmed upregulation of IL-6 in human HCC and suggested that it plays a central role in a gene expression network that drives tumor development (Ji et al., 2009). Elevated IL-6 was also found in viral and alcoholic hepatitis and liver cirrhosis, but in these conditions, IL-6 is expressed mainly by myeloid cells/leukocytes rather than parenchymal cells (Deviere et al., 1989; Kakumu et al., 1993; Soresi et al., 2006). Our studies indicate that the critical site of IL-6 expression shifts from myeloid cells to epithelial cells during the course of DEN-induced liver tumorigenesis. Initially, DEN administration rapidly induces IL-6 in Kupffer cells through NF-κB activation (Maeda et al., 2005). This initial surge in IL-6 is required for DEN-induced hepatocarcinogenesis (Naugler et al., 2007). Although IL-6 decays within 2 weeks of DEN administration, it reappears several months later, but at that time, it is expressed within FAH. IL-6 expression is also elevated in isolated HcPCs and is maintained in fully transformed HCC cells. Furthermore, autocrine IL-6 is important for HcPC to HCC progression and for tumorigenic growth. Autocrine IL-6 in both HcPC and HCC cells depends on elevated expression of LIN28, an RNA-binding protein that exerts its protumorigenic activity through downregulation of Let-7, an miRNA that inhibits IL-6 expression (Viswanathan and Daley, 2010). Accordingly, HcPCs exhibit downregulation of both Let-7f and Let-7g, and elevated LIN28 is found not only in isolated HcPCs but also within FAH and human HCV-induced dysplastic lesions.

A similar LIN28-Let-7-IL-6 epigenetic switch is important for in vitro programming and maintenance of cancer stem cells (Iliopoulos et al., 2009). IL-6 also induces malignant features in human ductal carcinoma stem cells (Sansone et al., 2007). In fact, autocrine IL-6 signaling was suggested to play a key role in STAT3-dependent tumor progression (Grivennikov and Karin, 2008). Another miRNA-driven autoregulatory circuit involved in

hepatocarcinogenesis accounts for elevated IL-6R expression (Hatziapostolou et al., 2011). Yet, HcPC-containing aggregates also express several other STAT3-activiting cytokines and receptors. Accordingly, silencing or ablation of IL-6 results in incomplete inhibition of HcPC to HCC progression. Nonetheless, our results demonstrate that autoregulatory circuits/epigenetic switches play an important role in the very early stages of tumorigenesis. Given that such circuits are already activated in premalignant cells, pharmacological agents that disrupt their function may be useful in cancer prevention. Prevention is of particular importance in cancers such as HCC, which is often detected at a stage that is refractory to currently available therapeutics.

EXPERIMENTAL PROCEDURES

Mice, HCC Induction, HcPC Isolation, and Transplantation

MUP-uPA transgenic mice (Weglarz et al., 2000) were maintained on a pure BL/6 background. Because homozygous females frequently die when pregnant, MUP-uPA heterozygotes were generated by backcrossing homozygous MUP-uPA males with BL/6 females to be used as recipients for hepatic transplantation. *Tak1*$^{\Delta hep}$ (Inokuchi et al., 2010) and *Il6*$^{F/F}$ (Quintana et al., 2013) mice were also in the BL/6 background. *Il6*$^{\Delta hep}$ mice were generated by crossing *Il6*$^{F/F}$ and *Alb-Cre* mice. C57BL/6 actin-GFP mice were from the Jackson Laboratories. BL/6 mice were purchased from Charles River Laboratories.

To induce HCC, 15-day-old mice were injected i.p. with 25 mg/kg DEN (Sigma). A pool of DEN-injected BL/6 mice was maintained and used in most experiments. Hepatocytes were isolated using a two-step procedure (He et al., 2010). Cell aggregates were isolated by filtration through 70 and 40 μm sieves. To disperse the aggregates into single cells, they were subjected to gentle pipetting in Ca/Mg-free PBS on ice. Single-cell suspensions of aggregated and nonaggregated hepatocytes were transplanted via an i.s. injection into 21-day-old male MUP-uPA mice (He et al., 2010). Alternatively, single-cell suspensions of aggregated hepatocytes were enriched for CD44^{+} HcPC using magnetic beads. As few as 100 viable CD44^{+} cells mixed with 1 × 10^{5} normal hepatocytes from normal males were transplanted into MUP-uPA mice. Alternatively, BL/6 mice were pretreated with retrorsine (70 mg/kg i.p.) (Sigma), a cell-cycle inhibitor, 1 month prior to transplantation. Transplanted mice were allowed to recover for 1 week and then injected weekly with 3× 0.5 ml/kg CCl_4 i.p. to induce liver injury and hepatocyte proliferation (Guo et al., 2002). Mice were sacrificed 5 to 6 months later, and tumors bigger than 1 mm in diameter on the liver surface were counted. Tumors bigger than 5 mm across were dissected for biochemical and molecular analyses.

ACCESSION NUMBERS

Raw gene expression array data have been deposited to NCBI's Gene Expression Omnibus under the GSE50431 study.

SUPPLEMENTAL INFORMATION

Supplemental Information includes Extended Experimental Procedures, seven figures, and three tables and can be found with this article online at http://dx.doi.org/10.1016/j.cell.2013.09.031.

AUTHOR CONTRIBUTIONS

G.H. identified, isolated, and characterized HcPCs; D.D. and H.N. optimized the HcPC isolation and purification procedure; D.D. found the mechanism of their dependence on autocrine IL-6 controlled by LIN28, characterized them using flow cytometry (with S.S.), and conducted miR analyses (with M.H. and D.I.); H.N. and D.D. used *Il6*$^{\Delta hep}$ mice to demonstrate in vivo HCC dependency on autocrine IL-6; H.N. (with R.T. and K.K.) found IL-6, LIN28, and P-STAT3 in human dysplastic lesions; J.F.-B. conducted the transcriptome analysis and exome sequencing (with S.E.Y., K.J., and O.H.) and with H.O. examined oncogenic potential of oval cells; H.O. examined HcPC proliferative potential and performed IF analysis of isolated HcPC (with A.S. and R.M.H.); Y.J. assisted with IHC and ISH staining; E.S. contributed to the experiments involving *Tak1*$^{\Delta hep}$ mice; G.H., D.D., J.F.-B., H.O., and M.K. wrote the manuscript.

ACKNOWLEDGMENTS

We acknowledge the Biogem facility at UCSD for their assistance with transcriptome analysis and A. Arian, K. Iwaisako, Y. Hiroshima, and H. Matsui for technical assistance. We thank Dr. J. Hidalgo (Universitat Autonoma de Barcelona, Spain) for the *Il6*$^{F/F}$ mice. Research was supported by the Superfund Basic Research Program (P42ES010337), NIH (CA118165 and CA155120), Wellcome Trust (WT086755), American Diabetes Association (7-08-MN-29), the Center for Translational Science (UL1RR031980 and UL1TR000100), the National Center for Research Resources IMAT program (N12R1CA155615), and postdoctoral research fellowships from the Damon Runyon Cancer Research Foundation (G.H.), American Liver Foundation (D.D.), Daiichi Sankyo Foundation of Life Science (H.N.), California Institute for Regenerative Medicine Stem Cell Training Grant II (TG2-01154) fellowship (J.F.-B.), Kanzawa Medical Research Foundation (H.O.), the German Research Foundation (DFG, SH721/1-1 to S.S.), and a Young Investigator Award from the National Childhood Cancer Foundation, "CureSearch" (D.D.). M.K. is an ACS Research Professor and is a recipient of the Ben and Wanda Hildyard Chair for Mitochondrial and Metabolic Diseases.

Received: December 11, 2012
Revised: June 4, 2013
Accepted: September 19, 2013
Published: October 10, 2013

REFERENCES

Bannasch, P. (1984). Sequential cellular changes during chemical carcinogenesis. J. Cancer Res. Clin. Oncol. *108*, 11–22.

Bladt, F., Riethmacher, D., Isenmann, S., Aguzzi, A., and Birchmeier, C. (1995). Essential role for the c-met receptor in the migration of myogenic precursor cells into the limb bud. Nature *376*, 768–771.

Deviere, J., Content, J., Denys, C., Vandenbussche, P., Schandene, L., Wybran, J., and Dupont, E. (1989). High interleukin-6 serum levels and increased production by leucocytes in alcoholic liver cirrhosis. Correlation with IgA serum levels and lymphokines production. Clin. Exp. Immunol. *77*, 221–225.

Dorrell, C., Erker, L., Schug, J., Kopp, J.L., Canaday, P.S., Fox, A.J., Smirnova, O., Duncan, A.W., Finegold, M.J., Sander, M., et al. (2011). Prospective isolation of a bipotential clonogenic liver progenitor cell in adult mice. Genes Dev. *25*, 1193–1203.

Duncan, A.W., Dorrell, C., and Grompe, M. (2009). Stem cells and liver regeneration. Gastroenterology *137*, 466–481.

Eferl, R., Ricci, R., Kenner, L., Zenz, R., David, J.P., Rath, M., and Wagner, E.F. (2003). Liver tumor development. c-Jun antagonizes the proapoptotic activity of p53. Cell *112*, 181–192.

El-Serag, H.B. (2011). Hepatocellular carcinoma. N. Engl. J. Med. *365*, 1118–1127.

Grivennikov, S., and Karin, M. (2008). Autocrine IL-6 signaling: a key event in tumorigenesis? Cancer Cell *13*, 7–9.

Guichard, C., Amaddeo, G., Imbeaud, S., Ladeiro, Y., Pelletier, L., Maad, I.B., Calderaro, J., Bioulac-Sage, P., Letexier, M., Degos, F., et al. (2012). Integrated analysis of somatic mutations and focal copy-number changes identifies key genes and pathways in hepatocellular carcinoma. Nat. Genet. *44*, 694–698.

Guo, D., Fu, T., Nelson, J.A., Superina, R.A., and Soriano, H.E. (2002). Liver repopulation after cell transplantation in mice treated with retrorsine and carbon tetrachloride. Transplantation *73*, 1818–1824.

Guo, X., Xiong, L., Sun, T., Peng, R., Zou, L., Zhu, H., Zhang, J., Li, H., and Zhao, J. (2012). Expression features of SOX9 associate with tumor progression and poor prognosis of hepatocellular carcinoma. Diagn. Pathol. *7*, 44.

Haridass, D., Yuan, Q., Becker, P.D., Cantz, T., Iken, M., Rothe, M., Narain, N., Bock, M., Nörder, M., Legrand, N., et al. (2009). Repopulation efficiencies of adult hepatocytes, fetal liver progenitor cells, and embryonic stem cell-derived hepatic cells in albumin-promoter-enhancer urokinase-type plasminogen activator mice. Am. J. Pathol. *175*, 1483–1492.

Hatziapostolou, M., Polytarchou, C., Aggelidou, E., Drakaki, A., Poultsides, G.A., Jaeger, S.A., Ogata, H., Karin, M., Struhl, K., Hadzopoulou-Cladaras, M., and Iliopoulos, D. (2011). An HNF4α-miRNA inflammatory feedback circuit regulates hepatocellular oncogenesis. Cell *147*, 1233–1247.

He, G., Yu, G.Y., Temkin, V., Ogata, H., Kuntzen, C., Sakurai, T., Sieghart, W., Peck-Radosavljevic, M., Leffert, H.L., and Karin, M. (2010). Hepatocyte IKKbeta/NF-kappaB inhibits tumor promotion and progression by preventing oxidative stress-driven STAT3 activation. Cancer Cell *17*, 286–297.

Hruban, R.H., Maitra, A., Kern, S.E., and Goggins, M. (2007). Precursors to pancreatic cancer. Gastroenterol. Clin. North Am. *36*, 831–849, vi.

Hytiroglou, P., Park, Y.N., Krinsky, G., and Theise, N.D. (2007). Hepatic precancerous lesions and small hepatocellular carcinoma. Gastroenterol. Clin. North Am. *36*, 867–887, vii.

Ichinohe, N., Kon, J., Sasaki, K., Nakamura, Y., Ooe, H., Tanimizu, N., and Mitaka, T. (2012). Growth ability and repopulation efficiency of transplanted hepatic stem cells, progenitor cells, and mature hepatocytes in retrorsine-treated rat livers. Cell Transplant. *21*, 11–22.

Iliopoulos, D., Hirsch, H.A., and Struhl, K. (2009). An epigenetic switch involving NF-kappaB, Lin28, Let-7 MicroRNA, and IL6 links inflammation to cell transformation. Cell *139*, 693–706.

Inokuchi, S., Aoyama, T., Miura, K., Osterreicher, C.H., Kodama, Y., Miyai, K., Akira, S., Brenner, D.A., and Seki, E. (2010). Disruption of TAK1 in hepatocytes causes hepatic injury, inflammation, fibrosis, and carcinogenesis. Proc. Natl. Acad. Sci. USA *107*, 844–849.

Ji, J., Shi, J., Budhu, A., Yu, Z., Forgues, M., Roessler, S., Ambs, S., Chen, Y., Meltzer, P.S., Croce, C.M., et al. (2009). MicroRNA expression, survival, and response to interferon in liver cancer. N. Engl. J. Med. *361*, 1437–1447.

Kakumu, S., Shinagawa, T., Ishikawa, T., Yoshioka, K., Wakita, T., and Ida, N. (1993). Interleukin 6 production by peripheral blood mononuclear cells in patients with chronic hepatitis B virus infection and primary biliary cirrhosis. Gastroenterol. Jpn. *28*, 18–24.

Kang, J.S., Wanibuchi, H., Morimura, K., Gonzalez, F.J., and Fukushima, S. (2007). Role of CYP2E1 in diethylnitrosamine-induced hepatocarcinogenesis in vivo. Cancer Res. *67*, 11141–11146.

Laconi, E., Oren, R., Mukhopadhyay, D.K., Hurston, E., Laconi, S., Pani, P., Dabeva, M.D., and Shafritz, D.A. (1998). Long-term, near-total liver replacement by transplantation of isolated hepatocytes in rats treated with retrorsine. Am. J. Pathol. *153*, 319–329.

Maeda, S., Kamata, H., Luo, J.L., Leffert, H., and Karin, M. (2005). IKKbeta couples hepatocyte death to cytokine-driven compensatory proliferation that promotes chemical hepatocarcinogenesis. Cell *121*, 977–990.

Marquardt, J.U., and Thorgeirsson, S.S. (2010). Stem cells in hepatocarcinogenesis: evidence from genomic data. Semin. Liver Dis. *30*, 26–34.

Meyer, K., Lee, J.S., Dyck, P.A., Cao, W.Q., Rao, M.S., Thorgeirsson, S.S., and Reddy, J.K. (2003). Molecular profiling of hepatocellular carcinomas developing spontaneously in acyl-CoA oxidase deficient mice: comparison with liver tumors induced in wild-type mice by a peroxisome proliferator and a genotoxic carcinogen. Carcinogenesis *24*, 975–984.

Mikhail, S., and He, A.R. (2011). Liver cancer stem cells. Int. J. Hepatol. *2011*, 486954.

Naugler, W.E., Sakurai, T., Kim, S., Maeda, S., Kim, K., Elsharkawy, A.M., and Karin, M. (2007). Gender disparity in liver cancer due to sex differences in MyD88-dependent IL-6 production. Science *317*, 121–124.

Nguyen, L.V., Vanner, R., Dirks, P., and Eaves, C.J. (2012). Cancer stem cells: an evolving concept. Nat. Rev. Cancer *12*, 133–143.

Nowell, P.C. (1976). The clonal evolution of tumor cell populations. Science *194*, 23–28.

Park, E.J., Lee, J.H., Yu, G.Y., He, G., Ali, S.R., Holzer, R.G., Osterreicher, C.H., Takahashi, H., and Karin, M. (2010). Dietary and genetic obesity promote liver inflammation and tumorigenesis by enhancing IL-6 and TNF expression. Cell *140*, 197–208.

Pitot, H.C. (1990). Altered hepatic foci: their role in murine hepatocarcinogenesis. Annu. Rev. Pharmacol. Toxicol. *30*, 465–500.

Porta, C., De Amici, M., Quaglini, S., Paglino, C., Tagliani, F., Boncimino, A., Moratti, R., and Corazza, G.R. (2008). Circulating interleukin-6 as a tumor marker for hepatocellular carcinoma. Ann. Oncol. *19*, 353–358.

Quintana, A., Erta, M., Ferrer, B., Comes, G., Giralt, M., and Hidalgo, J. (2013). Astrocyte-specific deficiency of interleukin-6 and its receptor reveal specific roles in survival, body weight and behavior. Brain Behav. Immun. *27*, 162–173.

Rabes, H.M. (1983). Development and growth of early preneoplastic lesions induced in the liver by chemical carcinogens. J. Cancer Res. Clin. Oncol. *106*, 85–92.

Rhim, J.A., Sandgren, E.P., Degen, J.L., Palmiter, R.D., and Brinster, R.L. (1994). Replacement of diseased mouse liver by hepatic cell transplantation. Science *263*, 1149–1152.

Sansone, P., Storci, G., Tavolari, S., Guarnieri, T., Giovannini, C., Taffurelli, M., Ceccarelli, C., Santini, D., Paterini, P., Marcu, K.B., et al. (2007). IL-6 triggers malignant features in mammospheres from human ductal breast carcinoma and normal mammary gland. J. Clin. Invest. *117*, 3988–4002.

Seki, S., Sakaguchi, H., Kitada, T., Tamori, A., Takeda, T., Kawada, N., Habu, D., Nakatani, K., Nishiguchi, S., and Shiomi, S. (2000). Outcomes of dysplastic nodules in human cirrhotic liver: a clinicopathological study. Clin. Cancer Res. *6*, 3469–3473.

Sell, S., and Leffert, H.L. (2008). Liver cancer stem cells. J. Clin. Oncol. *26*, 2800–2805.

Shin, S., Walton, G., Aoki, R., Brondell, K., Schug, J., Fox, A., Smirnova, O., Dorrell, C., Erker, L., Chu, A.S., et al. (2011). Foxl1-Cre-marked adult hepatic progenitors have clonogenic and bilineage differentiation potential. Genes Dev. *25*, 1185–1192.

Soresi, M., Giannitrapani, L., D'Antona, F., Florena, A.M., La Spada, E., Terranova, A., Cervello, M., D'Alessandro, N., and Montalto, G. (2006). Interleukin-6 and its soluble receptor in patients with liver cirrhosis and hepatocellular carcinoma. World J. Gastroenterol. *12*, 2563–2568.

Su, Y., Kanamoto, R., Miller, D.A., Ogawa, H., and Pitot, H.C. (1990). Regulation of the expression of the serine dehydratase gene in the kidney and liver of the rat. Biochem. Biophys. Res. Commun. *170*, 892–899.

Su, Q., Benner, A., Hofmann, W.J., Otto, G., Pichlmayr, R., and Bannasch, P. (1997). Human hepatic preneoplasia: phenotypes and proliferation kinetics of foci and nodules of altered hepatocytes and their relationship to liver cell dysplasia. Virchows Arch. *431*, 391–406.

Takayama, T., Makuuchi, M., Hirohashi, S., Sakamoto, M., Okazaki, N., Takayasu, K., Kosuge, T., Motoo, Y., Yamazaki, S., and Hasegawa, H. (1990). Malignant transformation of adenomatous hyperplasia to hepatocellular carcinoma. Lancet *336*, 1150–1153.

Terris, B., Cavard, C., and Perret, C. (2010). EpCAM, a new marker for cancer stem cells in hepatocellular carcinoma. J. Hepatol. *52*, 280–281.

Tsutsumi, M., Lasker, J.M., Shimizu, M., Rosman, A.S., and Lieber, C.S. (1989). The intralobular distribution of ethanol-inducible P450IIE1 in rat and human liver. Hepatology *10*, 437–446.

Verna, L., Whysner, J., and Williams, G.M. (1996). N-nitrosodiethylamine mechanistic data and risk assessment: bioactivation, DNA-adduct formation, mutagenicity, and tumor initiation. Pharmacol. Ther. *71*, 57–81.

Viswanathan, S.R., and Daley, G.Q. (2010). Lin28: A microRNA regulator with a macro role. Cell *140*, 445–449.

Wang, R., Ferrell, L.D., Faouzi, S., Maher, J.J., and Bishop, J.M. (2001). Activation of the Met receptor by cell attachment induces and sustains hepatocellular carcinomas in transgenic mice. J. Cell Biol. *153*, 1023–1034.

Weglarz, T.C., Degen, J.L., and Sandgren, E.P. (2000). Hepatocyte transplantation into diseased mouse liver. Kinetics of parenchymal repopulation and identification of the proliferative capacity of tetraploid and octaploid hepatocytes. Am. J. Pathol. *157*, 1963–1974.

Wood, L.D., Parsons, D.W., Jones, S., Lin, J., Sjöblom, T., Leary, R.J., Shen, D., Boca, S.M., Barber, T., Ptak, J., et al. (2007). The genomic landscapes of human breast and colorectal cancers. Science *318*, 1108–1113.

Yamashita, T., Forgues, M., Wang, W., Kim, J.W., Ye, Q., Jia, H., Budhu, A., Zanetti, K.A., Chen, Y., Qin, L.X., et al. (2008). EpCAM and alpha-fetoprotein expression defines novel prognostic subtypes of hepatocellular carcinoma. Cancer Res. *68*, 1451–1461.

Yang, Z.F., Ho, D.W., Ng, M.N., Lau, C.K., Yu, W.C., Ngai, P., Chu, P.W., Lam, C.T., Poon, R.T., and Fan, S.T. (2008). Significance of CD90+ cancer stem cells in human liver cancer. Cancer Cell *13*, 153–166.

Zheng, T., Wang, J., Jiang, H., and Liu, L. (2011). Hippo signaling in oval cells and hepatocarcinogenesis. Cancer Lett. *28*, 91–99.

Zhu, Z., Hao, X., Yan, M., Yao, M., Ge, C., Gu, J., and Li, J. (2010). Cancer stem/progenitor cells are highly enriched in CD133+CD44+ population in hepatocellular carcinoma. Int. J. Cancer *126*, 2067–2078.

Zöller, M. (2009). Tetraspanins: push and pull in suppressing and promoting metastasis. Nat. Rev. Cancer *9*, 40–55.

SCIENTIFIC REPORTS

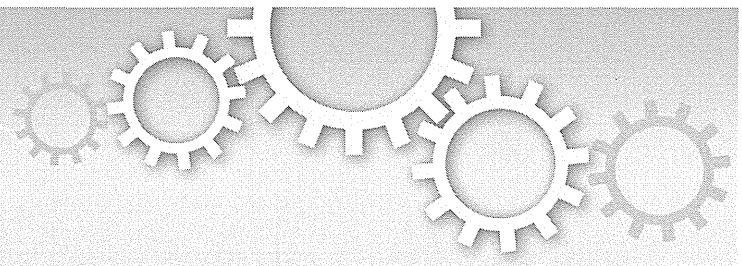

OPEN

SUBJECT AREAS:
TUMOUR IMMUNOLOGY
CANCER PREVENTION
LIVER CANCER
TRANSLATIONAL RESEARCH

Received
2 May 2013

Accepted
4 September 2013

Published
24 September 2013

Correspondence and requests for materials should be addressed to M.O. (otsukamo-tky@umin.ac.jp)

* These authors contributed equally to this work.

Regulation of the expression of the liver cancer susceptibility gene MICA by microRNAs

Takahiro Kishikawa[1]*, Motoyuki Otsuka[1,2]*, Takeshi Yoshikawa[1], Motoko Ohno[1], Akemi Takata[1], Chikako Shibata[1], Yuji Kondo[1], Masao Akanuma[3], Haruhiko Yoshida[1] & Kazuhiko Koike[1]

[1]Department of Gastroenterology, Graduate School of Medicine, The University of Tokyo, Tokyo 113-8655, Japan, [2]Japan Science and Technology Agency, PRESTO, Kawaguchi, Saitama 332-0012, Japan, [3]Division of Gastroenterology, The Institute for Adult Diseases, Asahi Life Foundation, Tokyo 100-0005, Japan.

Hepatocellular carcinoma (HCC) is a threat to public health worldwide. We previously identified the association of a single nucleotide polymorphism (SNP) at the promoter region of the MHC class I polypeptide-related sequence A (MICA) gene with the risk of hepatitis-virus-related HCC. Because this SNP affects MICA expression levels, regulating MICA expression levels may be important in the prevention of HCC. We herein show that the microRNA (miR) 25-93-106b cluster can modulate MICA levels in HCC cells. Overexpression of the miR 25-93-106b cluster significantly suppressed MICA expression. Conversely, silencing of this miR cluster enhanced MICA expression in cells that express substantial amounts of MICA. The changes in MICA expression levels by the miR25-93-106b cluster were biologically significant in an NKG2D-binding assay and an *in vivo* cell-killing model. These data suggest that the modulation of MICA expression levels by miRNAs may be a useful method to regulate HCCs during hepatitis viral infection.

Hepatocellular carcinoma (HCC) is the third most common cause of cancer-related mortality worldwide[1]. Although multiple major risk factors have been identified, such as genetic factors, environmental toxins, alcohol abuse, obesity, and metabolic disorders[2], infection with hepatitis virus B (HBV) or C (HCV) remains the major etiological factor for HCC[1].

Disease progression in HBV-induced or HCV-induced HCC is a multistep phenomenon. The clinical outcomes vary among individuals[1,3,4] because disease progression is influenced by both environmental and genetic risk factors. In terms of genetic susceptibility factors for HCV-induced HCC, we previously identified a single nucleotide polymorphism (SNP) site in the 5′-flanking region of the MICA gene on 6p21.33 (rs2596452) that is strongly associated with progression from chronic hepatitis C to HCC[5]. Individuals with the risk allele A of rs2596452 showed lower serum MICA protein levels[5]. Our subsequent study revealed that the same SNP site was also significantly associated with the risk of HBV-induced HCC[6]. However, interestingly, the risk allele was G in cases of HBV infection, which differed from HCV infection, and the individuals with the risk allele showed increased MICA protein expression levels[6]. Despite the different risk alleles at the same SNP site and inverse association between serum MICA levels and HCC risks in these two etiologies, MICA protein expression levels are significantly associated with susceptibility to HCC in chronic hepatitis viral infection.

MICA is highly expressed on viral-infected and cancer cells and acts as a ligand for NKG2D to activate the antitumor effects of natural killer cells and CD8 T cells[7,8]. This NKG2D-mediated tumor rejection is considered to be effective in the early stages of tumor growth[9–11]. Thus, the expression levels of MICA on the tumor cell surface may determine the antitumor efficacy, and the levels of shedding MICA in serum may act as a decoy of NKG2D to avoid tumor rejection.

Although several stress pathways regulate the transcription of the MICA gene[12,13], cellular microRNAs are suggested to control MICA protein expression via post-transcriptional mechanisms[14,15]. Recently, nucleic-acid-mediated gene therapy has been undergoing clinical trials[16]. Therefore, to target the clinical application of our GWAS results toward prevention of chronic-hepatitis-infection-induced HCC by nucleic-acid-mediated therapy, we determined the regulatory mechanisms of MICA protein expression using miRNA overexpression and miRNA functional silencing.

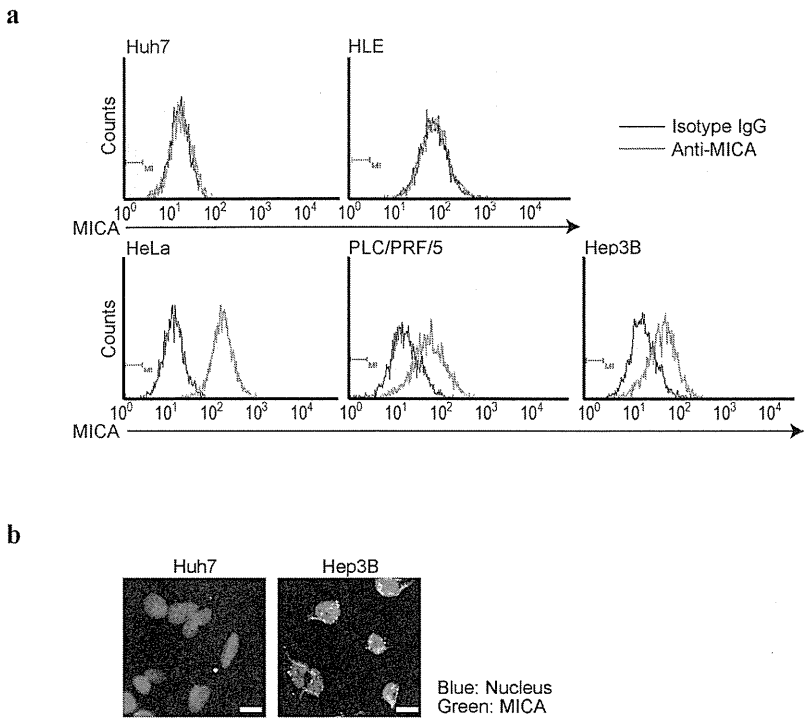

Figure 1 | Expression of MICA protein in HCC cells. (a), Flow cytometry assessment of MICA protein expression in HCC cells (purple lines). Isotype IgG was used for background staining (black lines). HeLa cells were used as the positive control. Representative results from two independent experiments are shown. (b), Immunofluorescence staining for MICA in Huh7 and Hep3B cells. Representative images from two independent experiments are shown. Scale bar, 25 μm.

Results

HCC cell lines differentially express MICA protein. To determine MICA protein levels in HCC cells, four representative HCC cell lines (Huh7, HLE, PLC/PRF/5, and Hep3B cells) underwent flow cytometry to evaluate MICA protein expression because no appropriate antibodies against MICA protein are at present available for western blotting. HeLa cells, which are known to express MICA protein[17], were used as a positive control. Hep3B and PLC/PRF/5 cells expressed substantial MICA protein levels, Huh7 and HLE cells expressed no MICA protein (Figure 1a). This was confirmed by immunocytochemistry using Huh7 and Hep3B cells, which showed staining mainly of cell surfaces (Figure 1b). These results suggest that the MICA protein expression status depends on the cell line examined, even those from the same organ.

The MiR25-93-106b cluster regulates MICA expression. Because upregulation of MICA expression was observed in Dicer-knockdown cells[18], we hypothesized that MICA expression levels may be at least partly regulated by miRNAs. We initially tested miRNAs that might affect MICA expression using reporter constructs into which MICA 3′-untranslated region (3′UTR) sequences were cloned and by transiently overexpressing 76 mature synthetic microRNAs, which were selected on the basis of their hepatic expression level, as in our previous studies[19,20]. Among the microRNAs examined, several may target MICA 3′UTR (Supplementary Figure 1). Among them, we focused on miR93 and miR106b, which were considered to target MICA 3′UTR based partly on the results of our initial miRNA testing described above; in addition, their possible target sequences were identified in the MICA 3′UTR sequences by a computational search using TargetScan 6.0 [21]. Additional reasons that we focused on these two miRNAs were as follows: 1) these miRNAs share the same seed sequences, to which two perfect-match complementary sequences exist in the 3′UTR of MICA (Figure 2a); 2) the target sequences are highly conserved among mammals and are thus likely to be biologically important sites; and 3) these miRNAs are located as a "miR25-93-106b cluster" on human chromosome 7q22.1, and so they may be expressed together under the same transcriptional control. We introduced mutations in the first possible miRNA target sequences of MICA 3′UTR in the reporter constructs (Supplementary Figure 2a); these sequences have a higher likelihood to be target sites, as determined by TargetScan. Co-transfection experiments revealed that reporter activity was suppressed by overexpression of a miR25-93-106b cluster-expressing plasmid (Figure 2b and Supplementary Figure 2b). The overexpression of an unrelated miR (let-7g)-expressing plasmid did not have any significant effects on the reporter activity (Supplementary Figure 2c) and the suppressive effect was lost using constructs with three point mutations in the seed sequences (Figure 2c), suggesting that miR25-93-106b directly targets these sequences and suppresses gene expression.

To confirm these effects, we generated HeLa and Hep3B cell lines that stably expressed the miR25-93-106b-cluster by transducing cells with miR25-93-106b-cluster-expressing lentiviruses (Figure 2d). As expected, the expression of the miR25-93-106b-cluster significantly suppressed MICA protein expression (Figure 2e). However, the expression levels of endogenous miR93 and 106b were not always proportional to the levels of MICA protein expression in the cell lines examined (Supplementary Figure 3). These results suggest that MICA protein expression can be regulated by miR93 and 106b, but that its expression is simultaneously endogenously regulated by other factors (possibly by promoter activities, including epigenetic changes).

Inhibition of miR25-93-106b function increases MICA protein expression. To develop methods of enhancing MICA protein expression levels based on the above results, we examined the

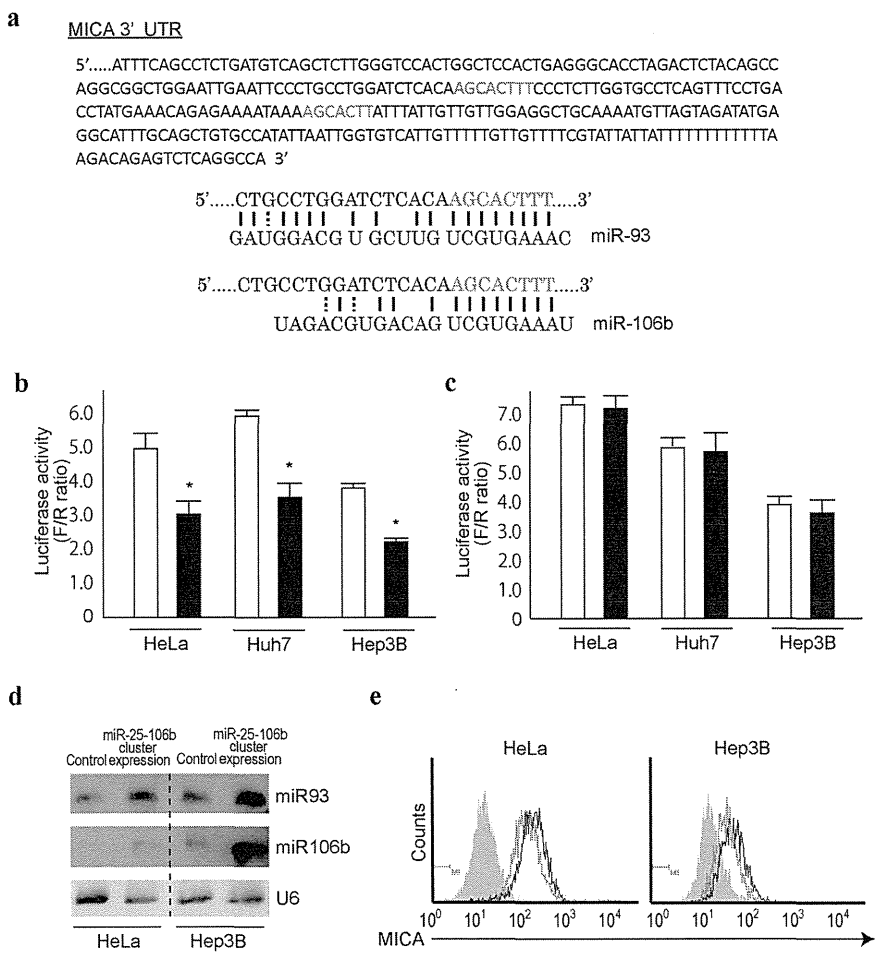

Figure 2 | miR93 and 106b target MICA 3′UTR. (a), *Sequences of MICA 3′UTR (upper). Letters in red are the sequences completely matched with the* seed regions of miR93 and 106b. The complementarities between the first predicted target in the MICA 3′UTR and miRNA sequences are shown below. (b), (c), Cells were co-transfected with pGL4-TK (renilla luciferase as an internal control), Luc-MICA-3′UTRwt (b) or Luc-MICA-3′UTRmut (c), and either an empty control vector (white bar) or miR25-93-106b-cluster expression plasmid (black bar). Data shows the means ± s.d. of the raw ratios (F/R) obtained by dividing firefly luciferase values with renilla luciferase values of three independent experiments. $*p < 0.05$. (d), miR93 and miR106b expression levels in control and stably miR25-93-106b cluster-expressing cells were determined by northern blotting. U6 levels were used as a loading control. Representative images from two independent experiments are shown. Full-length blot images are available in Supplementary Figure 5. (e), Suppression of MICA expression by overexpression of miRNA93 and 106b. Flow cytometry assessment of MICA protein expression in control (black lines) and stably miR25-93-106b cluster-expressing HeLa and Hep3B cells (red lines). Gray-shaded histograms represent the background staining using isotype IgG. Representative results from two independent experiments are shown.

effects of functional downregulation of miR25-93-106b on MICA expression. We first performed a reporter assay of transient functional silencing of miR25-93-106b using a construct that produces mature anti-sense RNAs designed to silence miR25-93-106b function. As expected, the reporter activities with MICA 3′UTR sequences were enhanced by the functional silencing of miR25-93-106b in HeLa, Hep3B, and Huh7 cells (Figure 3a). However, such effects were not observed using mutant reporter constructs not targeted by those miRNAs (Figure 3b), suggesting that the enhancing effects of the reporter activities were miRNA-dependent.

Next, HeLa, Hep3B, and Huh7 cells were stably transduced with a lentivirus that expresses anti-sense RNAs as described above, and MICA protein expression levels were determined by flow cytometry. Consistent with the reporter assay results, MICA protein expression was increased in HeLa and Hep3B cells by the functional silencing of miR25-93-106b (Figure 3c). However, in Huh7 cells, which express no MICA protein in the normal state, silencing of miR25-93-106b had no effect on MICA protein expression (Figure 3c). These results suggest that MICA protein expression levels can be regulated by modulating miRNA function, albeit only if at least a small quantity of MICA protein is present. In contrast, modulation of miRNA function does not influence MICA protein expression levels when the MICA protein is not expressed, but this could be because there are other forms of regulation at extremely low levels.

MICA protein levels are related to tumor susceptibility to NK cells. To determine the consequences of the modulation of MICA protein expression levels by miRNAs, we first determined the binding ability of NKG2D, a receptor of MICA, using HeLa and Hep3B cells overexpressing the miR25-93-106b cluster or with silencing of miR25-93-106b function. As expected, the levels of NKG2D binding to the cells, theoretically through binding to MICA, were decreased in HeLa and Hep3B cells overexpressing the miR25-93-106b cluster (Figure 4a). On the contrary, the levels of NKG2D binding to the cells were increased in HeLa and Hep3B cells in which miR25-93-106b function had been silenced (Figure 4b).

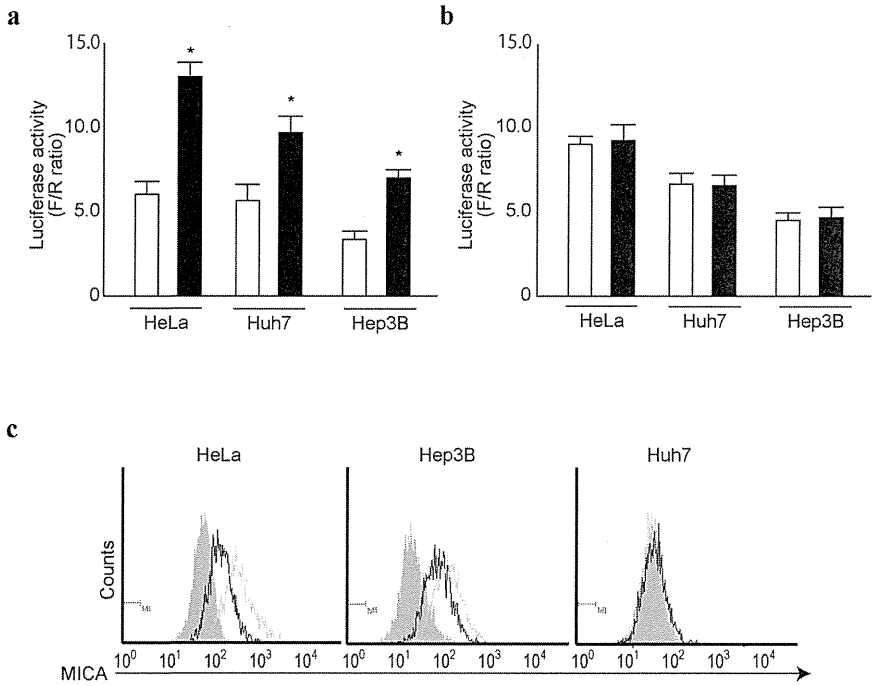

Figure 3 | Silencing of miR25-93-106b cluster enhances MICA expression. (a), (b), Cells were co-transfected with pGL4-TK (internal control), Luc-MICA-3′UTRwt (a) or Luc-MICA-3′UTRmut (b), and either an empty control vector (white bar) or plasmid expressing mature anti-sense sequences of miR25-93-106b cluster (black bar). Data shows the means ± s.d. of the raw ratios (F/R) obtained by dividing firefly luciferase values with renilla luciferase values of three independent experiments. $*p < 0.05$. (c), Enhancement of MICA expression by expression of anti-sense sequences of the miR25-93-106b cluster. Flow cytometry assessment of MICA protein expression in control (black lines) and stably mature anti-sense sequences of miR25-93-106b cluster-expressing cells (green lines). Gray-shaded histograms represent the background staining using isotype IgG. Representative results from three independent experiments are shown.

Next, to determine whether tumor cells with different miRNA-induced MICA protein expression levels exhibited differing susceptibilities to NK-cell-mediated killing *in vivo*, we performed a tumor-clearance assay that measures short-term *in vivo* killing by NK cells[22]. Hep3B control cells, Hep3B cells with miR25-93-106b cluster overexpression, or Hep3B cells with miR25-93-106b and HA-tagged MICA overexpression, labeled with fluorescent DiO, were injected into C57Black6/J mouse tail veins together with an equal number of HeLa cells labeled with Dil (internal reference control). After 5 h, surviving Hep3B and HeLa cells in the lungs were enumerated by flow cytometry. The number of Hep3B cells that had survived divided by the number of HeLa cells that had survived represents the relative killing of Hep3B cells *in vivo*. As shown by the *in vitro* binding assay using NKG2D, the killing rate of Hep3B cells in which miRNA function had been silenced was higher, and that of cells overexpressing miRNAs was lower, than that of control cells. The effects of miRNA overexpression were similar to those obtained in MICA knocked-down Hep3B cells (supplementary Figure 4). Additionally, the lower cell-killing rate in Hep3B cells overexpressing miRNA was antagonized by the co-expression of exogenous MICA protein (Figure 4c), suggesting that the decreased clearance was mediated by reduced MICA expression levels secondary to overexpression of miRNAs. These results suggest that tumor progression and invasion can be regulated by expression or silencing of miRNAs in at least some cells by regulation of MICA expression levels.

Discussion

In this study, we showed that the miR25-93-106b cluster modulates MICA protein expression by HCC cells. Because our previous GWAS analyses identified that MICA is the critical gene determining HCC susceptibility in patients with chronic hepatitis infection[5,6], the herein-described methods of modulating MICA expression may be useful for developing novel methods of prevention and therapeutics against HCCs.

MICA is a membrane protein that acts as a ligand for NKG2D to activate innate anti-tumor effects through natural killer and $CD8^+$ cells[7]. Our previous GWAS study showed that a risk allele at the SNP in the MICA promoter region was significantly associated with the susceptibility of HCV-induced HCC as well as with lower serum MICA levels. Although polymorphisms at the same SNP site were also associated with HBV-induced HCC, the risk allele determining the susceptibility of HCC was somehow different from that in HCV-induced HCC. While the reason why different MICA gene variations act as risk alleles at the same SNP site between HBV- and HCV-induced HCC has not been elucidated, it is assumed that changes in the membrane-bound MICA and soluble MICA levels due to differences in post-translational processing according to virus type may affect the risk allele results. In any case, because the importance of the regulation of MICA expression levels to prevent development of HCC due to chronic hepatitis viral infection cannot be denied, the regulation of MICA levels by microRNAs as shown here may be useful for the development of preventive methods of preventing HCC development during chronic hepatitis infection.

While several cellular signaling pathways lead to upregulation of MICA[12,13], we used microRNAs to regulate the expression levels of MICA in this study. As shown by the results of our GWAS analyses, which found that the polymorphisms in the promoter region of MICA are associated with changes in the sMICA levels[5,6], promoter activities of the MICA gene also have significant effects on MICA expression levels[23]. Our results showed that miR93 and 106b expression levels were not always correlated with those of MICA in HCC cell lines, suggesting that the regulation of MICA expression is not solely

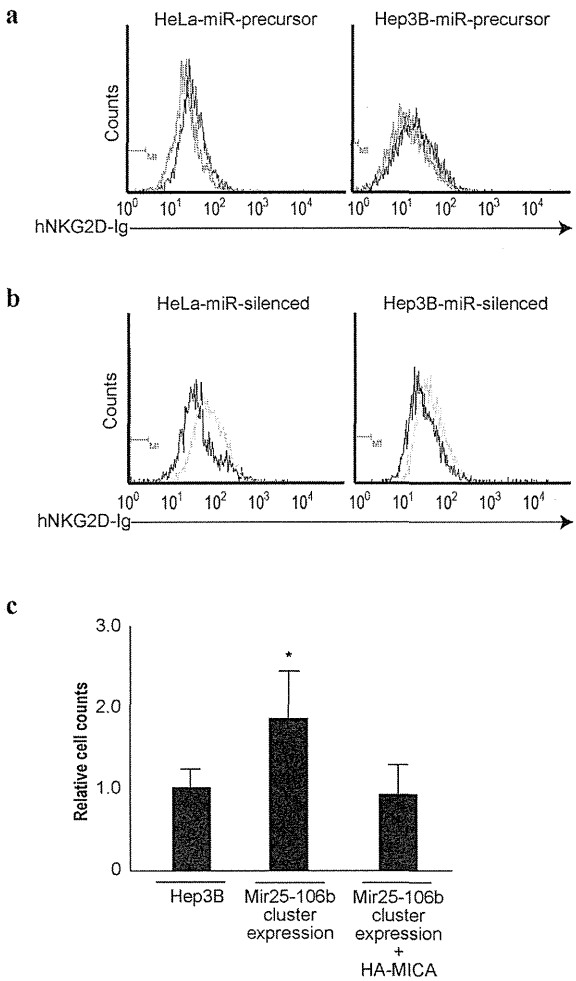

Figure 4 | NKG2D binding levels change in proportion to MICA expression levels. (a), (b), Flow cytometry of human IgG-fused NKG2D binding to the control (black lines), miR25-93-106b cluster-expressing cells (red lines) (a), and mature anti-sense sequences of miR25-93-106b cluster-expressing cells (green lines) (b). Representative results from three independent experiments are shown. (c), *In vivo* killing of DiO-labeled Hep3B and Dil-labeled HeLa cells (internal control cells) injected together into the tail veins of six mice in each group. Fluorescence intensities were quantified by flow cytometry as the ratio of Hep3B to HeLa cells in the lungs. The data from control Hep3B cells were set as 1.0. Data represent the means ± s.d. of three independent experiments. $*p < 0.05$.

dependent on miRNAs. In addition, in cells with no endogenous MICA expression, such as Huh7 cells, modulation of microRNA expression had no effect on the regulation of MICA expression. This suggests that at least low-level endogenous expression, which may be determined by promoter activities, are needed for regulation by miRNA. Therefore, changes in promoter activities and epigenetic changes in the MICA gene should also be determined. This will facilitate application of the regulatory function of miRNAs reported here.

One class of antisense oligonucleotides, namely locked nucleic acids, can be used to sequester microRNAs in the liver of various animals, including humans[16,24,25]. A clinical trial targeting miR-122 with the anti-miR-122 oligonucleotides miravirsen, the first miRNA-targeted drug, is underway for the treatment of HCV infection[16]. Thus, nucleic-acid-mediated gene therapy is becoming a realistic option. Modulation of MICA expression levels by such nucleic-acid-mediated therapy based on the results presented herein may also be a promising option for prevention and/or therapy of HCC.

In summary, we have shown that the miR25-93-106b cluster can be used to modulate MICA expression levels in HCC cells. Based on our GWAS results and associated studies, regulation of MICA protein expression levels is crucial to prevent the development of HCC during chronic hepatitis viral infection. It is important to identify the other factors that regulate MICA transcriptional activities as well as the post-translational processes and their association with susceptibility to HCCs. That said, miRNA regulation of MICA expression as shown here may facilitate regulation of the host innate immune system in an HCC-suppressive manner during chronic hepatitis viral infection.

Methods

Cell culture. The human HCC cell lines Huh7, HLE, PLC/PRF/5, and Hep3B were obtained from the Japanese Collection of Research Bioresources (JCRB, Osaka, Japan). The human cervical cancer cell line HeLa was obtained from the American Type Culture Collection (ATCC, Rockville, MD). All cells were maintained in Dulbecco's modified Eagle's medium supplemented with 10% fetal bovine serum.

Mouse. Experimental protocols were approved by the Ethics Committee for Animal Experimentation at the Graduate School of Medicine, the University of Tokyo and the Institute for Adult Disease, Asahi Life Foundation, Japan and conducted in accordance with the Guidelines for the Care and Use of Laboratory Animals of the Department of Medicine, the University of Tokyo, and the Institute for Adult Disease, Asahi Life Foundation.

Flow cytometry. Cells were hybridized with anti-MICA (1 : 500; R&D Systems, Minneapolis, MN) and isotype control IgG (1 : 500; R&D Systems) in 5% BSA/1% sodium azide/PBS for 1 h at 4°C. After washing, cells were incubated with goat anti-mouse Alexa 488 (1 : 1000; Molecular Probes, Eugene, OR) for 30 min. Flow cytometry was performed and data analyzed using Guava Easy Cyte Plus (GE Healthcare, Little Chalfont, UK).

Reporter plasmid construction, transient transfections, and luciferase assays. The reporter plasmid for the analysis of the effects of miRNAs on MICA 3′UTR were constructed by subcloning the MICA 3′UTR sequences from pLightSwitch-MICA 3UTR (SwitchGear Genomics, Menlo Park, CA) into the pGL4.50 vector (Promega, Madison, WI) at the *FseI* site by the In-Fusion method (Clontech, Mountain View, CA) to insert the MICA 3′UTR sequences into the 3′-UTR of the firefly luciferase gene, which was under the control of the CMV promoter. The sequences of the primers were 5′-CTA GAG TCG GGG CGG CG GCC ATT TCA GCC TCT GAT GTC AGC-3′ and 5′-GTC TGC TCG AAG CGG CCG GCC TGG CCT GAG ACT CTG TCT TAA-3′. The resultant plasmid (Luc-MICA 3′UTRwt) was used as a template for the construction of mutant reporter plasmid (Luc-MICA 3′UTRmut), which carries three point mutations in the seed sequences of miR93 and 106b in the MICA 3′UTR, itself generated by a Quik Change II XL Site-directed Mutagenesis Kit (Stratagene, Heidelberg, Germany) according to the manufacturer's instructions. Transient transfection and reporter assays were performed as described previously[26].

Lentiviral constructs, viral production, and transduction. To generate a neomycin-resistant miR25-93-106b cluster-expressing lentiviral construct, copGFP in the pmiRNA25-93-106b cluster-expressing plasmid (System Biosciences, Mountain View, CA) was replaced with a neomycin resistant gene, which was subcloned from the pCDH-Neo vector (System Biosciences), at the *FseI* site. The primers used were 5′-GCT ACC GCT ACG AGG CCG GCC CAT GAT TGA ACA AGA TGG ATT GCA-3′ and 5′-TCG CCG ATC ACG CGG CCG GCC TCA GAA GAA CTC GTC AAG AAG GC-3′. To remove the copGFP region from pmiRZIP25-93-106b (System Biosciences), a construct expressing mature anti-sense sequences of the miR25-93-106b cluster, sequences coding the GFP gene were removed by excision with *XbaI* and *PstI* sites followed by connecting the cut ends with annealed oligonucleotides (5′-CTA GAC GCC ACC ATG CTG CA-3′ and 5′-GCA TGG TGG CGT-3′) to maintain the coding frame and the expression of the downstream puromycin-resistance gene. To generate HA-tagged MICA protein overexpressing the lentiviral construct, MICA cDNA was amplified by PCR using a Halo-tag-MICA–expressing plasmid (Promega, Madison, WI) as a template and cloned into a pCDH-puro vector (System Biosciences) at the *NotI* site. The primer sequences used were 5′-ATC GGA TCC GCG GCC GCA CCA TGT ACC CAT ACG ATG TTC CAG ATT ACG CTA TGG GGC TGG GCC CGG TC-3′ and 5′-AGA TCC TTC GCG GCC GCT TAG GCG CCC TCA GTG GAG C-3′. Let-7g precursor expressing plasmid was generated by inserting about 1,000 bp long PCR product around the let-7g genomic region into pCDH-puro vector using *Xba1* and *Not1* sites. The production and concentration of lentiviral particles were described previously[27]. shRNA against MICA-producing lentiviral particles with puromycin resistant gene were purchased from SantaCruz Biotechnology (sc-4924-V, Dallas, TX). Cells were transduced with lentiviruses using

polybrene (EMD Millipore, Billerica, MA). The selections were performed with 400 μg/mL G418 and 2 μg/mL (HeLa) or 6 μg/mL (Hep3B) puromycin.

Immunocytochemistry. Cells on two-well chamber slides were fixed with 4% paraformaldehyde. Fixed cells were probed with the primary MICA antibody (R&D Systems) for 1 h after blocking with 5% normal goat serum for 30 min. Cells probed with the MICA antibody were incubated with the secondary Alexa Fluor 488 goat anti-mouse antibody (Molecular Probes) for 30 min. Slides were mounted using VectaShield with DAPI (Vector Labs, Burlingame, CA).

Northern blotting of miRNAs. Northern blotting of miRNAs was performed as described previously[27]. Briefly, total RNA was extracted using TRIzol Reagent (Invitrogen, Carlsbad, CA) according to the manufacturer's instructions. Ten micrograms of RNA were resolved in denaturing 15% polyacrylamide gels containing 7 M urea in 1 × TBE and then transferred to a Hybond N+ membrane (GE Healthcare) in 0.25 × TBE. Membranes were UV-crosslinked and prehybridized in hybridization buffer. Hybridization was performed overnight at 42°C in ULTRAhyb-Oligo Buffer (Ambion) containing a biotinylated probe specific for miR93 (cta cct gca cga aca gca ctt tg) and 106b (atc tgc act gtc agc act tta), which had previously been heated to 95°C for 2 min. Membranes were washed at 42°C in 2 × SSC containing 0.1% SDS, and the bound probe was visualized using a BrightStar BioDetect Kit (Ambion). Blots were stripped by boiling in a solution containing 0.1% SDS and 5 mM EDTA for 10 min prior to rehybridization with a U6 probe (cac gaa ttt gcg tgt cat cct t).

miRNA library screening. To screen for miRNAs that target MICA 3′-UTR, synthetic miRNA mimics and reporter constructs were used as described previously[19,20]. Seventy-six types of synthetic mature miRNAs that are highly expressed in the liver[28] were custom-made (B-Bridge, Tokyo, Japan) and transfected by RNAi Max (Life Technologies, Carlsbad, CA) into Huh7 cells in 96-well plates that had been transfected 24 h before with Luc-MICA 3′UTRwt. The cells were then incubated for another 24 h. As negative controls, oligonucleotides of artificial sequences were applied[19]. The luciferase activities were measured using a GloMax 96 Microplate Luminometer (Promega). The experiments were performed in duplicate.

NKG2D binding assay. Cells were incubated with 4 μg of recombinant human NKG2D fused to human IgG1 Fc chimera protein. After washing, cells were incubated with an Alexa488-conjugated affinity purified F(ab')2 fragment of goat anti-human IgG (Jackson ImmunoResearch Laboratories, West Grove, PA). As a negative control, cells were incubated with only Alexa488 anti-human IgG. The intensity of the fluorescence was determined by flow cytometry.

***In vivo* cell-killing assay.** Hep3B cells and HeLa cells were labeled with the fluorescent dye VybrantDiO and DiI (Molecular Probes), respectively. Cells were mixed at a density of 2×10^7 in 1-ml PBS, and 200 μl was injected into the tail vein. Five hours later, lungs were collected, and single-cell suspensions were collected using a cell strainer. Fluorescence was assayed by flow cytometry, and the ratio of the experimental Hep3B cells to HeLa cells (internal control) was calculated.

Statistical analysis. Statistically significant differences between groups were determined using Student's *t*-test when variances were equal. When variances were unequal, Welch's *t*-test was used instead. *P*-values of < 0.05 were considered to indicate statistical significance.

1. El-Serag, H. B. Epidemiology of viral hepatitis and hepatocellular carcinoma. *Gastroenterology* **142**, 1264–1273 (2012).
2. Sherman, M. Hepatocellular carcinoma: New and emerging risks. *Dig Liver Dis* **42**, S215–222 (2010).
3. Arzumanyan, A., Reis, H. M. & Feitelson, M. A. Pathogenic mechanisms in HBV- and HCV-associated hepatocellular carcinoma. *Nat Rev Cancer* **13**, 123–135 (2013).
4. Urabe, Y. *et al.* A genome-wide association study of HCV-induced liver cirrhosis in the Japanese population identifies novel susceptibility loci at the MHC region. *J Hepatol* (2013).
5. Kumar, V. *et al.* Genome-wide association study identifies a susceptibility locus for HCV-induced hepatocellular carcinoma. *Nat Genet* **43**, 455–458 (2011).
6. Kumar, V. *et al.* Soluble MICA and a MICA variation as possible prognostic biomarkers for HBV-induced hepatocellular carcinoma. *PLoS One* **7**, e44743 (2012).
7. Maccalli, C., Scaramuzza, S. & Parmiani, G. TNK cells (NKG2D+ CD8+ or CD4+ T lymphocytes) in the control of human tumors. *Cancer Immunol Immunother* **58**, 801–808 (2009).
8. Jinushi, M. *et al.* Impairment of natural killer cell and dendritic cell functions by the soluble form of MHC class I-related chain A in advanced human hepatocellular carcinomas. *J Hepatol* **43**, 1013–1020 (2005).
9. Diefenbach, A., Jensen, E. R., Jamieson, A. M. & Raulet, D. H. Rae1 and H60 ligands of the NKG2D receptor stimulate tumour immunity. *Nature* **413**, 165–171 (2001).
10. Hayakawa, Y. Targeting NKG2D in tumor surveillance. *Expert Opin Ther Targets* **16**, 587–599 (2012).
11. Guerra, N. *et al.* NKG2D-deficient mice are defective in tumor surveillance in models of spontaneous malignancy. *Immunity* **28**, 571–580 (2008).
12. Bauer, S. *et al.* Activation of NK cells and T cells by NKG2D, a receptor for stress-inducible MICA. *Science* **285**, 727–729 (1999).
13. Eleme, K. *et al.* Cell surface organization of stress-inducible proteins ULBP and MICA that stimulate human NK cells and T cells via NKG2D. *J Exp Med* **199**, 1005–1010 (2004).
14. Yadav, D., Ngolab, J., Lim, R. S., Krishnamurthy, S. & Bui, J. D. Cutting edge: down-regulation of MHC class I-related chain A on tumor cells by IFN-gamma-induced microRNA. *J Immunol* **182**, 39–43 (2009).
15. Stern-Ginossar, N. & Mandelboim, O. An integrated view of the regulation of NKG2D ligands. *Immunology* **128**, 1–6 (2009).
16. Janssen, H. L. *et al.* Treatment of HCV Infection by Targeting MicroRNA. *N Engl J Med* **368**, 1685–94 (2013).
17. Salih, H. R., Rammensee, H. G. & Steinle, A. Cutting edge: down-regulation of MICA on human tumors by proteolytic shedding. *J Immunol* **169**, 4098–4102 (2002).
18. Tang, K. F. *et al.* Decreased Dicer expression elicits DNA damage and up-regulation of MICA and MICB. *J Cell Biol* **182**, 233–239 (2008).
19. Takata, A. *et al.* MicroRNA-22 and microRNA-140 suppress NF-κB activity by regulating the expression of NF-κB coactivators. *Biochem Biophys Res Commun* **411**, 826–831 (2011).
20. Yoshikawa, T. *et al.* Silencing of microRNA-122 enhances interferon-a signaling in the liver through regulating SOCS3 promoter methylation. *Sci. Rep.* **2**, 637 (2012).
21. Lewis, B. P., Burge, C. B. & Bartel, D. P. Conserved seed pairing, often flanked by adenosines, indicates that thousands of human genes are microRNA targets. *Cell* **120**, 15–20 (2005).
22. Gazit, R. *et al.* Lethal influenza infection in the absence of the natural killer cell receptor gene Ncr1. *Nat Immunol* **7**, 517–523 (2006).
23. Lo, P. H. *et al.* Identification of a Functional Variant in the MICA Promoter Which Regulates MICA Expression and Increases HCV-Related Hepatocellular Carcinoma Risk. *PLoS One* **8**, e61279 (2013).
24. Lanford, R. E. *et al.* Therapeutic silencing of microRNA-122 in primates with chronic hepatitis C virus infection. *Science* **327**, 198–201 (2010).
25. Elmén, J. *et al.* LNA-mediated microRNA silencing in non-human primates. *Nature* **452**, 896–899 (2008).
26. Kojima, K. *et al.* MicroRNA122 is a key regulator of α-fetoprotein expression and influences the aggressiveness of hepatocellular carcinoma. *Nat Commun* **2**, 338 (2011).
27. Takata, A. *et al.* MicroRNA-140 acts as a liver tumor suppressor by controlling NF-κB activity by directly targeting DNA methyltransferase 1 (Dnmt1) expression. *Hepatology* **57**, 162–170 (2013).
28. Krützfeldt, J. *et al.* Silencing of microRNAs in vivo with 'antagomirs'. *Nature* **438**, 685–689 (2005).

Acknowledgments

This work was supported by Grants-in-Aid from the Ministry of Education, Culture, Sports, Science and Technology, Japan (#25293076, #25460979, and #24390183) (to M.Otsuka, Y.K. and K.K.), by Health Sciences Research Grants of The Ministry of Health, Labour and Welfare of Japan (to K.K.), and by grants from the Okinaka Memorial Institute for Medical Research, the Liver Forum in Kyoto, and the Princess Takamatsu Cancer Research Fund (to M.Otsuka).

Author contributions

T.K., M. Otsuka and K.K. planned the research and wrote the paper. T.K., M. Otsuka, T.Y., M. Ohno, A.T., C.S. and Y.K. performed the majority of the experiments. M.A. and H.Y. supported several experiments and analyzed the data. K.K. supervised the entire project.

Additional information

Supplementary information accompanies this paper at http://www.nature.com/scientificreports

Competing financial interests: The authors declare no competing financial interests.

How to cite this article: Kishikawa, T. *et al.* Regulation of the expression of the liver cancer susceptibility gene MICA by microRNAs. *Sci. Rep.* 3, 2739; DOI:10.1038/srep02739 (2013).

Biochemical and Biophysical Research Communications 432 (2013) 22–27

Contents lists available at SciVerse ScienceDirect

Biochemical and Biophysical Research Communications

journal homepage: www.elsevier.com/locate/ybbrc

Overexpression of gankyrin in mouse hepatocytes induces hemangioma by suppressing factor inhibiting hypoxia-inducible factor-1 (FIH-1) and activating hypoxia-inducible factor-1

Yu Liu [a], Hiroaki Higashitsuji [a,*], Hisako Higashitsuji [a], Katsuhiko Itoh [a], Toshiharu Sakurai [b], Kazuhiko Koike [c], Kiichi Hirota [d], Manabu Fukumoto [e], Jun Fujita [a,*]

[a] Department of Clinical Molecular Biology, Graduate School of Medicine, Kyoto University, 54 Shogoin Kawaharacho, Sakyo-ku, Kyoto 606-8507, Japan
[b] Department of Gastroenterology and Hepatology, Faculty of Medicine, Kinki University, 377-2 Ohno-Higashi, Osaka-Sayama, Osaka 589-8511, Japan
[c] Department of Gastroenterology, Graduate School of Medicine, The University of Tokyo, 7-3-1 Hongo, Bunkyo-ku, Tokyo 113-8655, Japan
[d] Department of Anesthesia, Kyoto University Hospital, 54 Shogoin-Kawaracho, Sakyo-Ku, Kyoto 606-8507, Japan
[e] Department of Pathology, Institute of Development, Aging and Cancer, Tohoku University, Sendai 980-8575, Japan

ARTICLE INFO

Article history:
Received 22 January 2013
Available online 1 February 2013

Keywords:
PSMD10
HIF-1
FIH-1
Oncogene
Hemangioma

ABSTRACT

Gankyrin (also called p28 or PSMD10) is an oncoprotein commonly overexpressed in hepatocellular carcinomas. It consists of 7 ankyrin repeats and interacts with multiple proteins including Rb, Cdk4, MDM2 and NF-κB. To assess the oncogenic activity *in vivo*, we produced transgenic mice that overexpress gankyrin specifically in the hepatocytes. Unexpectedly, 5 of 7 F2 transgenic mice overexpressing hepatitis B virus X protein (HBX) promoter-driven gankyrin, and one of 3 founder mice overexpressing serum amyloid P component (SAP) promoter-driven gankyrin developed hepatic vascular neoplasms (hemangioma/hemangiosarcomas) whereas none of the wild-type mice did. Endothelial overgrowth was more frequent in the livers of diethylnitrosamine-treated transgenic mice than wild-type mice. Mouse hepatoma Hepa1-6 cells overexpressing gankyrin formed tumors with more vascularity than parental Hepa1-6 cells in the transplanted mouse skin. We found that gankyrin binds to and sequester factor inhibiting hypoxia-inducible factor-1 (FIH-1), which results in decreased interaction between FIH-1 and hypoxia-inducible factor-1α (HIF-1α) and increased activity of HIF-1 to promote VEGF production. The effects of gankyrin were more prominent under 3% O_2 than 1% or 20% O_2 conditions. Thus, the present study clarified, at least partly, mechanisms of vascular tumorigenesis, and suggests that gankyrin might play a physiological role in hypoxic responses besides its roles as an oncoprotein.

1. Introduction

Gankyrin (also called p28, p28^{GANK} or PSMD10) was identified as an oncoprotein commonly overexpressed in hepatocellular carcinomas (HCCs) [1]. Gankyrin was also independently isolated as p28, a supposed component of the 26S proteasome, but recent studies have demonstrated that p28 associates only with free 19S particles of the 26S proteasome or their precursors and functions as a chaperone to guide their assembly [2]. As expected for a protein consisting of 7 ankyrin repeats [3], gankyrin interacts with multiple proteins and shows a variety of activities. For example, gankyrin binds to Rb and Cdk4, and accelerates phosphorylation and degradation of Rb to activate DNA synthesis genes [1]. Gankyrin binds to the E3 ubiquitin ligase MDM2, thereby facilitating ubiquitylation and degradation of p53 [4]. Gankirin binds to NF-κB and suppresses its activity by modulating acetylation via SIRT1 [5]. Gankyrin binds to hepatocyte nuclear factor 4α, which determines hepatocyte differentiation status and enhances its degradation [6]. Gankyrin activates PI3K/AKT/mTOR/hypoxia-inducible factor-1 (HIF-1) signaling [7].

Most solid tumors contain hypoxic regions, and one of the most important cellular factors involved in the hypoxic response which promotes angiogenesis, anaerobic metabolism and resistance to apoptosis is HIF-1 [8,9]. HIF-1 is a heterodimeric transcription factor composed of a constitutively expressed β subunit and an inducibly expressed α subunit (HIF-1α). Under aerobic conditions, HIF-1α is hydroxylated by specific prolyl hydroxylases at two conserved Pro residues in a reaction requiring oxygen. Hydroxylation

Abbreviations: CAD, C-terminal transactivation domain; DEN, diethylnitrosamine; FIH-1, factor inhibiting hypoxia-inducible factor-1; firefly-luciferase, F-Luc; H&E, hematoxylin and eosin; HBX, hepatitis B virus X protein; HCC, hepatocellular carcinoma; HIF, hypoxia-inducible factor; RT-qPCR, reverse transcription-quantitative polymerase chain reaction; SAP, serum amyloid P component.

* Corresponding authors. Fax: +81 75 7514977.
E-mail addresses: hhigashi@virus.kyoto-u.ac.jp (H. Higashitsuji), jfujita@virus.kyoto-u.ac.jp (J. Fujita).

0006-291X/$ - see front matter © 2013 Elsevier Inc. All rights reserved.
http://dx.doi.org/10.1016/j.bbrc.2013.01.093

facilitates binding of von Hippel–Lindau protein, a component of the ubiquitin protein ligase, to HIF-1α, leading to its proteasomal degradation. The ability of HIF-1α to activate transcription is also prevented by factor inhibiting HIF-1 (FIH-1) [8–10]. FIH-1 hydroxylates a specific Asn residue in HIF-1α, and disrupts interaction of HIF-1α with the transcription co-activators p300 and CBP. Under hypoxic conditions, prolyl hydroxylase and FIH-1 activities are inhibited by substrate (O_2) deprivation, resulting in HIF-1α stabilization and binding to the p300/CBP complex, thus allowing HIF transactivation.

Since gankyrin plays important roles in cell proliferation and apoptosis, is overexpressed in most HCCs, and confers tumorigenicity to non-malignant cells, we produced transgenic mice that overexpressed gankyrin specifically in the hepatocytes to assess its oncogenic activity *in vivo*. Unexpectedly, the mice developed vascular tumors (hemangioma/hemangiosarcomas) in the liver, and so we have tried to elucidate the underlying mechanisms for vascularization.

2. Materials and methods

2.1. Transgenic mice

To express gankyrin specifically in the liver, cDNA for the mouse wild-type gankyrin N-terminally tagged with 2× FLAG was cloned into the pBEPBglII expression vector containing the hepatitis B virus X protein (HBX) promoter [11]. Fertilized eggs were obtained from C57BL/6J mice, and transgenic mice were produced at the Center for Animal Resources and Development, Kumamoto University, Japan. A plasmid containing the human serum amyloid P component (SAP) promoter [12] and expressing mouse wild-type gankyrin N-terminally tagged with 3× FLAG was also constructed, and transgenic mice were produced with this at the Genome Information Research Center, Osaka University, Japan, using eggs from D2B6F1 mice. For genotyping, DNA was extracted from the tail of each mouse and analyzed by Southern blotting using gankyrin cDNA as probe.

2.2. Treatment of mice

A single intraperitoneal injection of diethylnitrosamine (DEN, Sigma, 25 mg/kg of body weight) was administered to 14-days-old transgenic and control male mice. Groups of animals were euthanized at 8 months after injection, and the livers were removed, examined for visible lesions, and paraffin embedded after fixation in 10% buffered formalin.

For tumor formation, cells (2×10^6) were suspended in 0.1 ml of PBS and injected subcutaneously into the back of athymic BALB/c mice (Japan SLC Inc.). Each mouse received Hepa1-6 cells on one side and Hepa1-6/GK cells on the other side. All experiments involving mice were approved by the Animal Research Committee of Kyoto University, and conducted in accordance with the institutional and NIH guidelines for the care and use of laboratory animals.

2.3. Human materials

Eighteen specimens of HCC were taken by needle biopsy before initiation of the treatment at Kinki University Hospital, Japan. The study protocol was approved by the institutional review boards, and written informed consent was obtained from all patients for subsequent use of their collected tissues.

2.4. Cell culture and DNA transfection

U-2 OS cells, HEK293 cells, HEK293T cells, mouse hepatoma Hepa1-6 cells and their transfectants were maintained in Dulbecco's modified Eagle's medium supplemented with 10% fetal bovine serum at 37 °C and 5% CO_2 as described [4]. For mild hypoxic conditions, cells were placed in a modular incubator chamber and flushed with a gas mixture containing 1 or 3% O_2, 5% CO_2, and balance N2.

Calcium phosphate-DNA coprecipitation method was used for DNA transfection. Plasmids encoding, gankyrin, shRNA for gankyrin, HIF-1α, FIH-1, and their fusion proteins have been described previously [4,5,10,13].

2.5. Pathologicall analyses

The immunohistochemical staining was performed on 4-μm-thick paraffin sections of tissues fixed in 10% buffered formalin as described [14]. The sections were incubated with the primary antibodies against endothelial cell markers CD31 (dianoba GmbH) and CD34 (Abnova), followed by horseradish peroxidase-conjugated anti-rat immunoglobulin antibody (Santa Cruz Biotechnology), and were developed in Diaminobenzidine colorimetric reagent solution (DAKO). They were counterstained with hematoxylin. To assess the presence of the atypical proliferative lesion of endothelial cells, at least 1 section from 4 lobes were examined under a microscope.

2.6. Analyses of gene expression and protein interactions

Preparation of cell lysates, immunoprecipitation, and Western blot analysis were performed as described [4]. Rabbit polyclonal anti-gankyrin, anti-VEGF-A, anti-HIF-1α, anti-FIH-1, anti-β-actin, and biotin-conjugated anti-HA antibodies (all from Santa Cruz Biotech.), anti-Myc tag antibody (MBL), anti-FLAG and biotin-conjugated anti-FLAG antibodies (Sigma), mouse monoclonal anti-HA antibody (Roche), and rabbit polyclonal antibody raised against recombinant mouse gankyrin were used as the primary antibodies in Western blotting.

For immunoprecipitation, mouse anti-HA antibody (Roche), rabbit anti-FLAG antibody, and biotin-conjugated anti-FLAG and anti-HA antibodies were used.

Reverse transcription-quantitative polymerase chain reaction (RT-qPCR) analysis was done as described [14]. The relative levels of gankyrin and VEGF-A mRNAs were determined by RT-qPCR using β-actin and GAPDH mRNA for normalization. Primer sequences used were as follows: gankyrin (human, 5′-TCTTCAAGCCATCCTGTGTG-3′ and 5′-TGGTGATGTTGGACTCCTCA-3′), VEGF-A (human, 5′-AAAA CTGCT GGTGTCCCAAG-3′ and 5′-ATTAAACCCAGGCCACCTTT-3′; mouse, 5′-CA GGCTGCTGTAACGATGAA-3′ and 5′-TATGTGCTGGCTTTGGTGAG-3′), β-actin (human, CTACGTCGCCCTGGACTTCGAGC and GATGGAGC CGCCGATCCACACGG), GAPDH (mouse, 5′-ACAACTTTGTC AAGCT-CATTTCCTG-3′ and 5′-TGGTCCAGGGTTTCTTACTCCTTGG-3′).

2.7. Reporter assays

The reporter plasmids p2.1 and p2.4 contain wild-type and mutant copies, respectively, of the hypoxia response element (HRE) from the *ENO1* gene upstream of an SV40 promoter and firefly luciferase (F-Luc) coding sequences [13]. U-2 OS cells were cotransfected with either p2.1 or p2.4, pRL vector expressing Renilla luciferase (pRL-CMV, Promega) and plasmids expressing HA-FIH-1 and FLAG-gankyrin or gankyrin-shRNA [4].

The GAL4 reporter plasmid GAL4E1bLuc containing five GAL4-binding sites upstream of an E1b TATA sequence and the F-Luc gene, and GAL4-expressing plasmids GalA(531–826) and

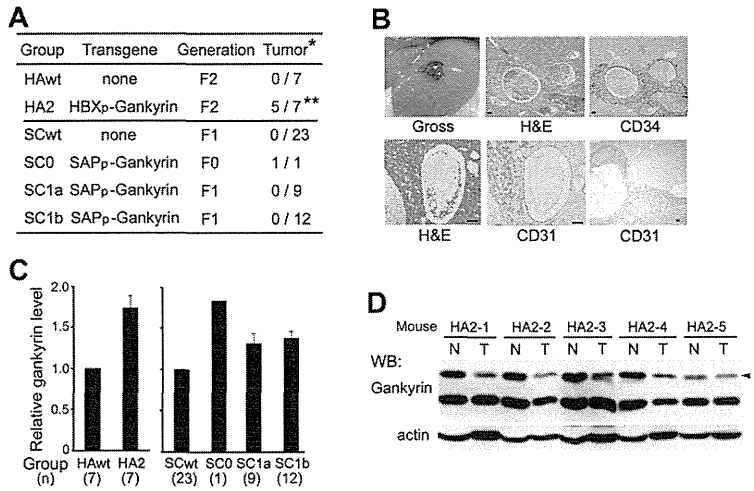

Fig. 1. Vascular tumors in gankyrin-transgenic mice. (A) Incidence of hepatic tumors. Gankyrin was expressed in hepatocytes by using HBX promoter (HBXp) or SAP promoter (SAPp). *number of mice with hepatic tumors at 22 months of age/total number of mice. **$P < 0.05$ compared with HAwt group. (B) Gross and microscopic appearances of hepatic vascular lesions in transgenic mice. H&E, hematoxylin and eosin staining. CD31 and CD34, immunoperoxidase staining for CD31 and CD34, respectively, using diaminobenzidine as substrate. Bar, 50 μm. (C) Gankyrin expression in the non-tumorous liver. Lysates prepared from indicated mice were analyzed by Western blotting and densitometry. Bars are average ± SD of total gankyrin levels normalized with actin levels, and expressed as relative to those of wild-type mice. (D) Expression of endogenous and exogenous (arrowhead) gankyrin in the tumor (T) and non-tumorous portion (N) of the liver from indicated F2 transgenic mice. Western blot analysis.

GalA-N803 expressing the C-terminal transactivation domain (CAD) of the wild-type and FIH-1-insensitive HIF-1α, respectively, fused to the GAL4 DNA-binding domain were described previously [15]. U-2 OS cells were cotransfected with GAL4E1bLuc, pRL-CMV, GAL4-expressing plasmids, and plasmids expressing FLAG-gankyrin or gankyrin-shRNA.

Transfected cells were exposed to mild hypoxia (1 or 3% O_2) for 48 h and harvested for dual luciferase assays (Promega) as described [5].

2.8. Statistical analysis

To determine whether the means of two groups are significantly different from each other, the Student's *t*-test and chi-square test were used. All statistical analyses including Fisher's exact probability test were performed using the JMP software (SAS Institute). A *P* value less than 0.05 was considered statistically significant.

3. Results

3.1. Vascular neoplasms developed in the liver of gankyrin-transgenic mouse

The HBX promoter [11] was first used to direct hepatocyte-specific expression of the wild-type gankyrin in transgenic mice. Two founder (F0) mice were obtained and subsequently mated with wild-type mice to produce F1 offspring containing the transgene. F1 mice were then mated with wild-type mice to produce F2 offspring. When F0, F1 and F2 mice were sacrificed at 9–13 months

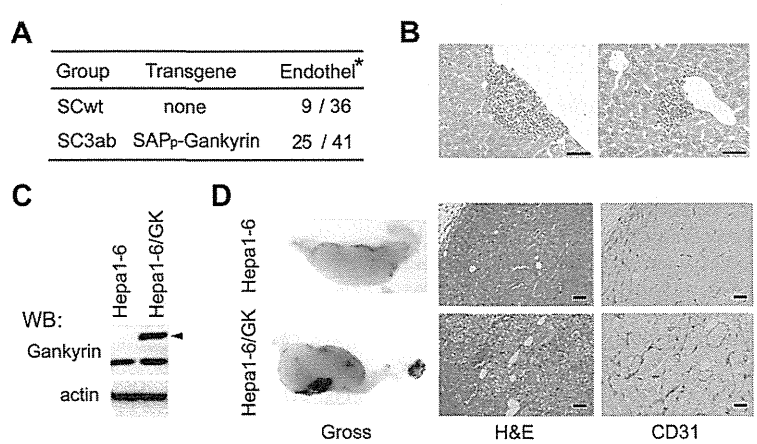

Fig. 2. Increased vascularity of hepatic tumors overexpressing gankyrin. (A) Vascularity in the livers of gankyrin-transgenic (SC3ab) and wild-type (SCwt) mice with diethylnitrosamine (DEN)-induced HCCs. Eight months after DEN treatment, mice were sacrificed and tumor vascularity was evaluated microscopically. *Number of mice with endothelial overgrowth in the liver/number of mice administered DEN. $P < 0.05$ between these groups. (B) Typical examples of atypical proliferation of endothelial cells in (A). H&E stain. Bar, 50 μm. (C) Expression of endogenous and exogenous (arrowhead) gankyrin in Hepa1-6 and Hepa1-6/GK cells analyzed by Western blotting. (D) Vascularity of Hepa1-6 and Hepa1-6/GK tumors in nude mouse skin. Typical gross and microscopic (H&E and immunoperoxidase staining of CD31) appearances of formalin-fixed paraffin-embedded tumors. Bar, 50 μm.

of age, no hepatic tumor was observed (data not shown). At 22 months of age, however, 5 of the remaining 7 male F2 developed hepatic vascular tumors, whereas no tumor was found in the control mice (Fig. 1A and B). The protein level of gankyrin in the non-tumorous liver of transgenic mice was about 1.7-fold compared with that of wild-type mice (Fig. 1C). The tumors consisted of large somewhat irregular vascular channels lined by endothelial cells. In some areas elongated or spindle-shaped endothelial cells lined vascular spaces, formed solid sheets, with an atypical nucleus, suggesting malignancy (Fig. 1B). Immunohisochemical analysis demonstrated that the tumor cells expressed the endothelial cell markers CD31 and CD34. The expression of gankyrin was less in the vascular tumors than non-tumorous liver tissues (Fig. 1D). Taken together, these results indicated that the observed tumors were hemangioma/hemangiosarcomas.

To increase the expression level of transgene in the liver, we next produced gankyrin-transgenic mice using the SAP promoter [12]. At the age of 22 months, one of the 3 F0 mice developed hemangioma/hemangiosarcomas, but none of its F1 offspring and other 2 F0 mice (Fig. 1A). In the F0 with vascular tumors, the transgene was integrated into more than one locus, resulting in inheritance of less integration sites and lower levels of gankyrin expression in the offspring (Fig. 1C and data not shown).

3.2. Increased vascularity in tumors overexpressing gankyrin

To evaluate the effect of gankyrin on angiogenesis in the liver, we used the DEN-induced hepatocarcinogenesis model. At 8 months after DEN treatment, 100% of wild-type mice and SAP promoter-driven gankyrin-transgenic mice (F4) developed hepatocarcinomas. Multiplicity of tumors was not different between the two groups, but the incidence of microscopic vascular lesions characterized by angiectasis and atypically proliferating endothelial cells was significantly higher in the transgenic mice than wild-type mice (Fig. 2A and B).

To further examine the effect of gankyrin on neovasculization, we stably overexpressed FLAG-tagged gankyrin in mouse Hepa1-6 hepatoma cells (Hepa1-6/GK cells, Fig. 2C). Two weeks after inoculation, both Hepa1-6 and Hepa1-6/GK cells formed tumors, and tumor vascularity was grossly more prominent in the Hepa1-6/GK tumors compared with Hepa1-6 tumors in all 6 mice inoculated (Fig. 2D). Immunohistochemical staining with anti-CD31 endothelial marker antibody demonstrated increased blood vessel density in Hepa1-6/GK tumors compared with Hepa1-6 tumors. Thus, overexpression of gankyrin increased the neovascularization.

3.3. Increased VEGF expression induced by gankyrin

Since HIF-1-mediated expression of VEGF stimulates angiogenesis [8,9], we analyzed expression of HIF-1α and VEGF-A. As shown in Fig. 3A, expression levels of VEGF-A protein and mRNA were higher in the livers of gankyrin-transgenic mice compared to wild-type mice. Overexpression of gankyrin in Hepa1-6 cells also increased protein level of VEGF-A, although the HIF-1α level was not increased. (Fig. 3B).

Transcriptional activation of the VEGF gene in response to hypoxia is mediated by binding of HIF-1 to HRE [13]. To examine whether gankyrin affects transcriptional activity mediated by HRE, we transfected U-2 OS cells with HRE-Luc reporter plasmid. Gankyrin enhanced the luciferase activity induced by mild hypoxia (3% O_2) by 4-fold, but only 1.5-fold or no enhancement at 1% or 20% O_2 concentration, respectively (Fig. 3C and data not shown). Conversely, suppression of gankyrin expression by shRNA reduced the luciferase activity. When HRE was mutated, the luciferase activity was not increased by hypoxia, and the enhancing effect

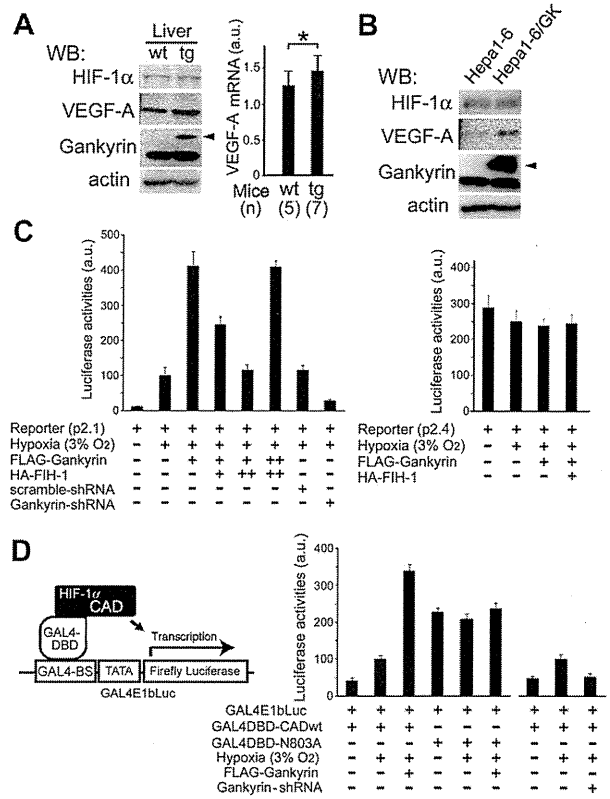

Fig. 3. Increased VEGF expression induced by gankyrin. (A) VEGF-A and HIF-1α expression in the livers of wild-type (wt) and gankyrin-transgenic (tg) mice. Western blotting (left) and RT-qPCR (right). Arrowhead, FLAG-Gankyrin. VEGF-A transcript levels were normalized with GAPDH levels. Values are average ± SD. $^*P < 0.05$. a.u., arbitrary unit. (B) Effects of gankyrin on expression of VEGF-A. Hepa1-6 cells and Hepa1-6 transfectants overexpressing FLAG-Gankyrin (Hepa1-6/GK) were analyzed by Western blotting. Arrowhead, FLAG-Gankyrin. (C) HRE-dependent transcriptional activation. U-2 OS cells were cotransfected with *ENO1*–F-luciferase (Luc) reporter plasmids (p2.1) or mutated reporter plasmids lacking the HIF-1 recognition sequence (p2.4), and plasmids expressing R-Luc, FLAG-Gankyrin, HA–FIH-1, gankyrin-shRNA, and scrambled-shRNA as indicated. 48 h later, some dishes were transferred to hypoxic conditions. After further 48-h incubation, cell lysates were analyzed for Luc activity. F-Luc activity was normalized with R-Luc activity. Values are average ± SD from 3 independent experiments. a.u., arbitrary unit. (D) Asn803-dependent increase in HIF-1α transcriptional activity. U-2 OS cells were cotransfected with Gal4–F-Luc reporter plasmids (GAL4E1bLuc), plasmids expressing GAL4 DNA-binding domain (DBD) fused to wild-type (wt) or N803A mutant C-terminal half (CAD) of HIF-1α, R-Luc, and FLAG-Gankyrin and gankyrin-shRNA as indicated. After 48 h of hypoxic incubation, Luc activities were measured and expressed as in (C). GAL4-BS, GAL4-binding sites. a.u., arbitrary unit.

of gankyrin was not observed, indicating that the effect was mediated by HRE.

We next examined whether gankyrin affects transcriptional activity of HIF-1α. We employed a reporter system composed of the F-Luc gene whose expression is controlled by GAL4-binding elements (GAL4E1bLuc, Fig. 3D) and the HIF1α-CAD fused to the GAL4 DNA-binding domain [13]. Compared with normoxia (20% O_2), luciferase activity was 2.5-fold higher at 3% O_2 concentration (Fig. 3D). Overexpression of gankyrin further increased the HIF-1α activity by 3-fold, whereas suppression of gankyrin reduced it. At 1% or 20% O_2 concentration, however, these effects of gankyrin were not observed (data not shown). When fusion protein of HIF-1α-CAD mutated at Asn803 was used, gankyrin showed no effect. Since Asn803 is the critical residue for FIH-1 to inhibit HIF-1α activity, these results suggest that the effect of gankyrin was mediated by FIH-1.

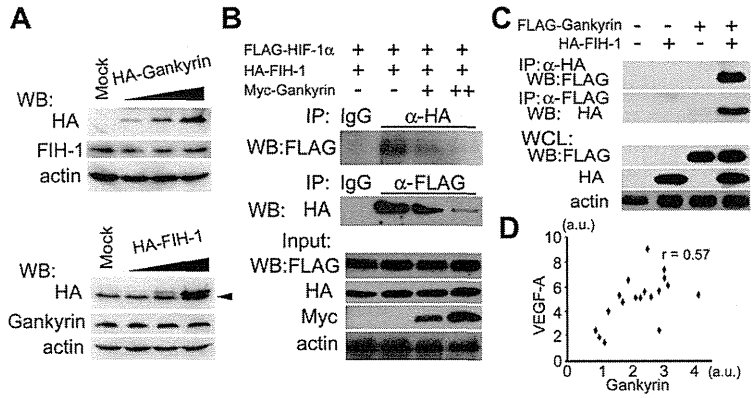

Fig. 4. Binding of gankyrin to FIH-1. (A) Effect of gankyrin on FIH-1 protein level. HEK293 cells were transfected with increasing amounts of plasmids expressing HA-gankyrin or HA-FIH-1, or empty vector (Mock) as indicated. 48 h later, cell lysates were analyzed by Western blotting. Arrowhead, non-specific bands. (B) Effect of gankyrin on binding of HIF-1α to FIH-1. HEK293T cells were cotransfected with plasmids expressing FLAG–HIF-1α, HA–FIH-1, and Myc-tag-gankyrin, and cultured at 3% O_2 for 48 h. Cell lysates were immunoprecipitated (IP), and precipitants and inputs were analyzed by Western blotting (WB) using the indicated antibodies. (C) Interaction of gankyrin with FIH-1. HEK293T cells were cotransfected with plasmids expressing FLAG-Gankyrin and HA-FIH-1, and cultured at 3% O_2 for 48 h. Cell lysates were immunoprecipitated, and precipitants and inputs were analyzed by WB as in (B). WCL, whole cell lysates. Experiments were repeated three times with similar results. (D) Scatter plot of mRNA levels of gankyrin and VEGF-A in human hepatocellular carcinoma specimens. a.u., arbitrary unit.

3.4. Sequestration and inhibition of FIH-1 by gankyrin

We examined whether or not gankyrin suppresses FIH-1 expression. Overexpression of gankyrin did not affect FIH-1 level (Fig. 4A). When FIH-1 was overexpressed, the gankyrin level did not change, either. Thus, we suspected that gankyrin might affect the interaction of FIH-1 and HIF-1α. As shown in Fig. 4B, binding of FIH-1 and HIF-1α was suppressed by gankyrin. As FIH-1 binds ankyrin repeat domain proteins [16] and gankyrin contains 7 ankyrin repeats [3], we checked the possibility that gankyrin binds to FIH-1. HA-FIH-1 and FLAG-gankyrin were coimmunoprecipitated by either anti-HA or anti-FLAG antibody from cells cultured at 3% O_2, but not or only slightly at 1% or 20% O_2 concentration, respectively (Fig. 4C and data not shown). These results demonstrate that gankyrin binds to and sequester FIH-1, resulting in decreased interaction between FIH-1 and HIF-1α and increased activity of HIF-1 under mild hypoxic conditions. When we further examined the mRNA levels of gankyrin and VEGF-A in biopsy specimens of human HCC, a moderate positive correlation ($r = 0.57$, $P < 0.02$) was found (Fig. 4D), suggesting that the gankyrin–FIH-1 interaction might have some clinical relevance.

4. Discussion

Hemangioma/hemangiosarcomas are occasionally seen in mouse liver with incidences less than 3% [17]. In the present study, 71% of the F2 transgenic mice overexpressing HBX promoter-driven gankyrin developed hepatic hemangioma/hemangiosarcomas, whereas none of the wild-type mice did. This phenotype was probably not due to random insertional mutagenesis in the transgenic mice as it was also observed in F0 mice expressing SAP promoter-driven gankyrin. In the subsequent generations of this F0, however, gankyrin levels were decreased and no hemangioma/hemangiosarcoma developed. The finding that mice with 70% increase, but none with 35% increase in the protein level of hepatic gankyrin developed hemangioma/hemangiosarcomas (Fig. 1C) suggests that there is a critical level of gankyrin to show this phenotype.

How does overexpression of gankyrin in hepatocytes induce endothelial cell-derived tumors? As gankyrin induces dedifferentiation of HCCs [6], it may also induce transdifferentiation of hepatocytes into endothelial cells. A more feasible explanation, however, would be that gankyrin facilitates a sustained release of angiogenic growth factors, providing the milieu leading to hemangiosarcoma formation [18]. Consistent with this notion, endothelial overgrowth was more frequent in the HCCs of gankyrin-transgenic mice than wild-type mice after DEN treatment. Furthermore, mouse hepatoma transfectants overexpressing gankyrin induced more neovasculalization than parental cells when subcutaneously inoculated into nude mice. VEGF-A was the first identified member of the VEGF family, and mice with transgenic VEGF-A expressed in the liver have increased vascularization and vascular permeability [19]. When myoblasts overexpressing VEGF-A are transplanted into limb or heart muscle of mice, they induce hemangiomas [20]. In the present study, VEGF-A level was higher in the liver of gankyrin-transgenic mice compared with wild-type mice, and gankyrin increased VEGF-A expression in cultured hepatoma cells. Thus, VEGF-A probably contributed to formation of hemangioma/hemangiosarcomas in the gankyrin-transgenic mice.

HIF-1 is a major factor regulating the level of VEGF, and despite induction of multiple angiogenic target genes such as adrenomedullin and placental growth factor, VEGF is essential for HIF-1 mediated neovascularization [21]. Hypoxia induces changes in the hydroxylation status of well-conserved Pro and Asn residues of HIF-1α, resulting in protein stabilization and transcriptional activation [8,9]. Signaling through receptor tyrosine kinases induce HIF-1 expression by increasing the rate of HIF-1α protein synthesis via PI3K/Akt/mTOR pathway [8], and gankyrin activates this to promote VEGF expression [7]. In the present study, the HIF-1α protein level was not increased in cells overexpressing gankyrin. Reporter assays indicated, however, that HIF-1 transcriptional activity was increased by gankyrin, and that it was dependent on Asn803 of HIF-1α. FIH-1 hydroxylates this residue and inhibits transcriptional activity [8–10]. In addition to HIF-1α, proteins containing ankyrin repeat domains are common targets for hydroxylation by FIH-1, and IκBα as well as Notch-1 block the FIH-1-mediated HIF-1α repression by sequestering FIH-1 [22]. In this case, the recognition of each substrate and their relative affinity for FIH-1 is an important determinant of FIH-1 sequestration and consequently HIF regulation. Consistent with the recent study using recombinant proteins [16], gankyrin and FIH-1 were co-immunoprecipitated from cell lysates. Furthermore, overexpression of gankyrin reduced the amount of HIF-1α bound to FIH-1, suggesting a higher affinity for FIH-1 of gankyrin than HIF-1α at mild hypoxia. As expected, gankyrin increased the HIF-1 transcriptional activity in reporter

assays, which was dependent on FIH-1. Interestingly, the binding of gankyrin to FIH-1 and enhancement of HIF-1 activity were dependent on the O_2 concentration.

We have demonstrated in this study that sustained overexpression of gankyrin in hepatocytes, although at a low level, can induce liver hemangioma/hemangiosarcomas in mice. Gankyrin sequesters FIH-1 from HIF-1α to activate HIF-1 and increase production of VEGF, which at least partly contributes to hemangioma/hemangiosarcoma formation. Further studies will clarify why spontaneous hemangioma/hemangiosarcomas are extremely rare in humans in contrast to experimental animals [18], and shed light on mechanisms of vascular tumorigenesis as well as hepatocarcinogeneis. The present study also suggests that gankyrin might play a physiological role in hypoxic responses besides its roles as an oncoprotein.

Acknowledgments

We thank Profs. R.J. Mayer, University of Nottingham, U.K. and Ryuzo Sakata, Kyoto University for helpful suggestions, and Ms. Fumiyo Kataoka for technical assistance. This work was partly supported by Grants-in-Aid for Scientific Research from the Ministry of Education, Culture, Sports, Science and Technology of Japan, the Japan Society for the Promotion of Science, Cooperative Research Project Program of IDAC, Tohoku University, Global COE Program "Center for Frontier Medicine", MEXT, Japan, and the Japan Smoking Research Foundation.

References

[1] H. Higashitsuji, K. Itoh, T. Nagao, et al., Reduced stability of retinoblastoma protein by gankyrin, an oncogenic ankyrin-repeat protein overexpressed in hepatomas, Nat. Med. 6 (2000) 96–99.
[2] H.C. Besche, A. Peth, A.L. Goldberg, Getting to first base in proteasome assembly, Cell 138 (2009) 25–28.
[3] S. Krzywda, A.M. Brzozowski, H. Higashitsuji, et al., The crystal structure of gankyrin, an oncoprotein found in complexes with cyclin-dependent kinase 4, a 19 S proteasomal ATPase regulator, and the tumor suppressors Rb and p53, J. Biol. Chem. 279 (2004) 1541–1545.
[4] H. Higashitsuji, H. Higashitsuji, K. Itoh, et al., The oncoprotein gankyrin binds to MDM2/HDM2, enhancing ubiquitylation and degradation of p53, Cancer Cell 8 (2005) 75–87.
[5] H. Higashitsuji, H. Higashitsuji, Y. Liu, et al., The oncoprotein gankyrin interacts with RelA and suppresses NF-kappaB activity, Biochem. Biophys. Res. Commun. 363 (2007) 879–884.
[6] W. Sun, J. Ding, K. Wu, et al., Gankyrin-mediated dedifferentiation facilitates the tumorigenicity of rat hepatocytes and hepatoma cells, Hepatology 54 (2011) 1259–1272.
[7] J. Fu, Y. Chen, J. Cao, et al., P28GANK overexpression accelerates hepatocellular carcinoma invasiveness and metastasis via phosphoinositol 3-kinase/AKT/hypoxia-inducible factor-1α pathways, Hepatology 53 (2011) 181–192.
[8] G.L. Semenza, HIF-1: upstream and downstream of cancer metabolism, Curr. Opin. Genet. Dev. 20 (2010) 51–56.
[9] M.Y. Koh, G. Powis, Passing the baton: the HIF switch, Trends Biochem. Sci. 37 (2012) 364–372.
[10] P.C. Mahon, K. Hirota, G.L. Semenza, FIH-1: a novel protein that interacts with HIF-1alpha and VHL to mediate repression of HIF-1 transcriptional activity, Genes Dev. 15 (2001) 2586–2675.
[11] K. Koike, K. Moriya, K. Ishibashi, et al., Expression of hepatitis C virus envelope proteins in transgenic mice, J. Gen. Virol. 76 (1995) 3031–3038.
[12] K. Araki, O. Hino, J. Miyazaki, K. Yamamura, Development of two types of hepatocellular carcinoma in transgenic mice carrying the SV40 large T-antigen gene, Carcinogenesis 12 (1991) 2059–2062.
[13] G.L. Semenza, B.H. Jiang, S.W. Leung, Hypoxia response elements in the aldolase A, enolase 1, and lactate dehydrogenase A gene promoters contain essential binding sites for hypoxia-inducible factor 1, J. Biol. Chem. 271 (1996) 32529–32537.
[14] A. Umemura, Y. Itoh, K. Itoh, et al., Association of gankyrin protein expression with early clinical stages and insulin-like growth factor-binding protein 5 expression in human hepatocellular carcinoma, Hepatology 47 (2008) 493–502.
[15] B.H. Jiang, J.Z. Zheng, S.W. Leung, et al., Transactivation and inhibitory domains of hypoxia-inducible factor 1alpha, J. Biol. Chem. 272 (1997) 19253–19260.
[16] S.E. Wilkins, S. Karttunen, R.J. Hampton-Smith, et al., Factor inhibiting HIF (FIH) recognizes distinct molecular features within hypoxia-inducible factor-α (HIF-α) versus ankyrin repeat substrates, J. Biol. Chem. 287 (2012) 8769–8781.
[17] T. Harada, A. Enomoto, G.A. Boorman, R.R. Maronpot, Liver and gallbladder, in: R.R. Maronpot (Ed.), Pathology of the Mouse, Cache River Press, Vienna, IL, 1999, pp. 119–183.
[18] S.M. Cohen, R.D. Storer, K.A. Criswell, et al., Hemangiosarcoma in rodents: mode-of-action evaluation and human relevance, Toxicol. Sci. 111 (2009) 4–18.
[19] P. Leppänen, I. Kholová, A.J. Mähönen, et al., Short and long-term effects of hVEGF-A(165) in Cre-activated transgenic mice, PLoS One 1 (2006) e13.
[20] M.L. Springer, A. Banfi, J. Ye, et al., Localization of vascular response to VEGF is not dependent on heparin binding, FASEB J. 21 (2007) 2074–2085.
[21] S. Oladipupo, S. Hu, J. Kovalski, et al., VEGF is essential for hypoxia-inducible factor-mediated neovascularization but dispensable for endothelial sprouting, Proc. Natl. Acad. Sci. USA 108 (2011) 13264–13269.
[22] D.H. Shin, S.H. Li, S.W. Yang, et al., Inhibitor of nuclear factor-kappaB alpha derepresses hypoxia-inducible factor-1 during moderate hypoxia by sequestering factor inhibiting hypoxia-inducible factor from hypoxia-inducible factor 1alpha, FEBS J. 276 (2009) 3470–3480.

Journal of Clinical Virology 57 (2013) 173–177

Contents lists available at SciVerse ScienceDirect

Journal of Clinical Virology

journal homepage: www.elsevier.com/locate/jcv

Case report

Uninodular combined hepatocellular and cholangiocarcinoma with multiple non-neoplastic hypervascular lesions appearing in the liver of a patient with HIV and HCV coinfection

Koji Uchino[a], Ryosuke Tateishi[a,*], Hayato Nakagawa[a], Junichi Shindoh[b], Yasuhiko Sugawara[b], Masaaki Akahane[c], Junji Shibahara[d], Haruhiko Yoshida[a], Kazuhiko Koike[a]

[a] Department of Gastroenterology, Graduate School of Medicine, The University of Tokyo, Tokyo, Japan
[b] The Artificial Organ and Transplantation Division, Department of Surgery, Graduate School of Medicine, The University of Tokyo, Tokyo, Japan
[c] Department of Radiology, Graduate School of Medicine, The University of Tokyo, Tokyo, Japan
[d] Department of Pathology, Graduate School of Medicine, The University of Tokyo, Tokyo, Japan

ARTICLE INFO

Article history:
Received 27 August 2012
Received in revised form 2 December 2012
Accepted 18 January 2013

Keywords:
Combined hepatocellular and cholangiocarcinoma
Human immunodeficiency virus
Hepatitis C virus
Highly active antiretroviral therapy

ABSTRACT

A 42-year-old man suffering from haemophilia A and coinfection of human immunodeficiency virus (HIV) and hepatitis C virus was referred to our institution because of multiple liver tumours. He had been receiving highly active antiretroviral therapy for HIV infection. Ultrasonography showed multiple hypoechoic space-occupying lesions in the liver. Contrast-enhanced dynamic computed tomography (CT) and magnetic resonance imaging revealed multiple ring-enhanced hypervascular lesions in the liver. An ultrasonography-guided biopsy was performed and histological evaluation indicated one of the lesions to be combined hepatocellular and cholangiocarcinoma and others to be non-neoplastic. The patient underwent partial hepatic resection and is currently alive without recurrence for 15 months. Multiple ring-enhanced lesions have been undetectable in postoperative follow-up CT examinations.

1. Why this case is important

Because of shared routes of viral transmission, coinfection with human immunodeficiency virus (HIV) and hepatitis C virus (HCV) is not uncommon.[1,2] As a result of advances in highly active antiretroviral therapy (HAART), the morbidity and mortality associated with HIV infection have declined. Instead, HCV-related liver disease, including cirrhosis and hepatocellular carcinoma (HCC), and hepatotoxic effects associated with antiretroviral drugs have become major problems for patients coinfected with HIV and HCV.[3] We report a case of multiple hepatic hypervascular lesions appearing in a patient coinfected with HIV and HCV, which were found to be solitary combined hepatocellular and cholangiocarcinoma (cHCC-CC) accompanied by non-neoplastic lesions.

2. Case report

A 42-year-old man suffering from haemophilia A and coinfection of HIV and HCV was referred to our institution because of liver tumours. He had been examined periodically with ultrasonography but no liver tumours had been detected until then. The patient had been treated with atazanavir, ritonavir and tenofovir disoproxil/emtricitabine for HIV infection and remained asymptomatic. He did not take any medicine including herbal medicines other than the antiviral drugs described above. Blood-test results at the referral were: albumin, 3.7 g dl^{-1}; total bilirubin, 3.1 mg dl^{-1}; direct bilirubin, 1.1 mg dl^{-1}; aspartate aminotransferase, 65 IU l^{-1}; alanine aminotransferase, 44 IU l^{-1}; alkaline phosphatase, 623 IU l^{-1}; gamma-glutamyl transpeptidase, 149 IU l^{-1}; platelet count, 122×10^3 μl^{-1}; international normalised ratio of prothrombin time, 0.93; alpha-foetoprotein (AFP), 73 ng ml^{-1}; lens culinaris agglutinin-reactive fraction of AFP, 5.6%; des-gamma-carboxy prothrombin, 28 mAU ml^{-1}; carcinoembryonic antigen, 3.0 ng ml^{-1}; carbohydrate antigen 19-9, 119 U ml^{-1}; and CD4 count 177 cells μl^{-1}. HIV1-RNA was not detectable and HCV-RNA was 7.2 Log IU ml^{-1}. Blood culture was negative. Ultrasonography showed multiple hypoechoic lesions in the liver with a maximum diameter of 1.8 cm (Fig. 1A–C). One nodule in the segment 5 was more sharply marginated than other

Abbreviations: AFP, alpha-foetoprotein; cHCC-CC, combined hepatocellular and cholangiocarcinoma; CT, computed tomography; Gd-EOB-DTPA, gadolinium-ethoxybenzyl-diethylenetriamine pentaacetic acid; HAART, highly active antiretroviral therapy; HCC, hepatocellular carcinoma; HCV, hepatitis C virus; HIV, human immunodeficiency virus; MRI, magnetic resonance imaging.

* Corresponding author at: Department of Gastroenterology, Graduate School of Medicine, The University of Tokyo, 7-3-1 Hongo, Bunkyo-ku, Tokyo 113-8655, Japan. Tel.: +81 3 3815 5411; fax: +81 3 3814 0021.
E-mail address: tateishi-tky@umin.ac.jp (R. Tateishi).

1386-6532/$ – see front matter © 2013 Elsevier B.V. All rights reserved.
http://dx.doi.org/10.1016/j.jcv.2013.01.012

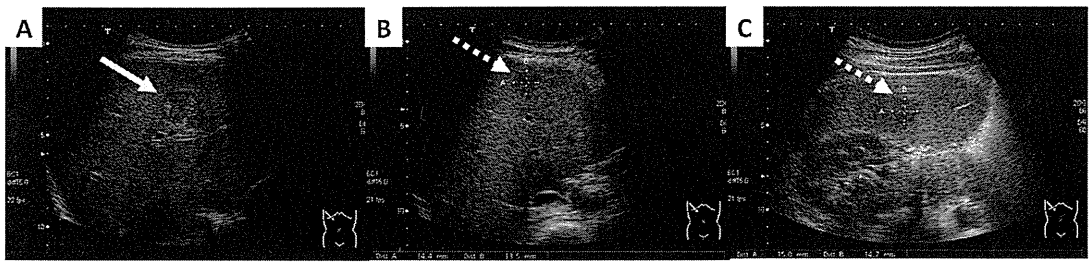

Fig. 1. Ultrasonography showing multiple hypoechoic lesions in the liver. The nodule in segment 5 was diagnosed pathologically as cHCC-CC, which was more sharply-marginated than other nodules, with mosaic pattern internal echo (Panel A, arrow). The other lesions were nonneoplastic (Panel B and C, dotted arrow).

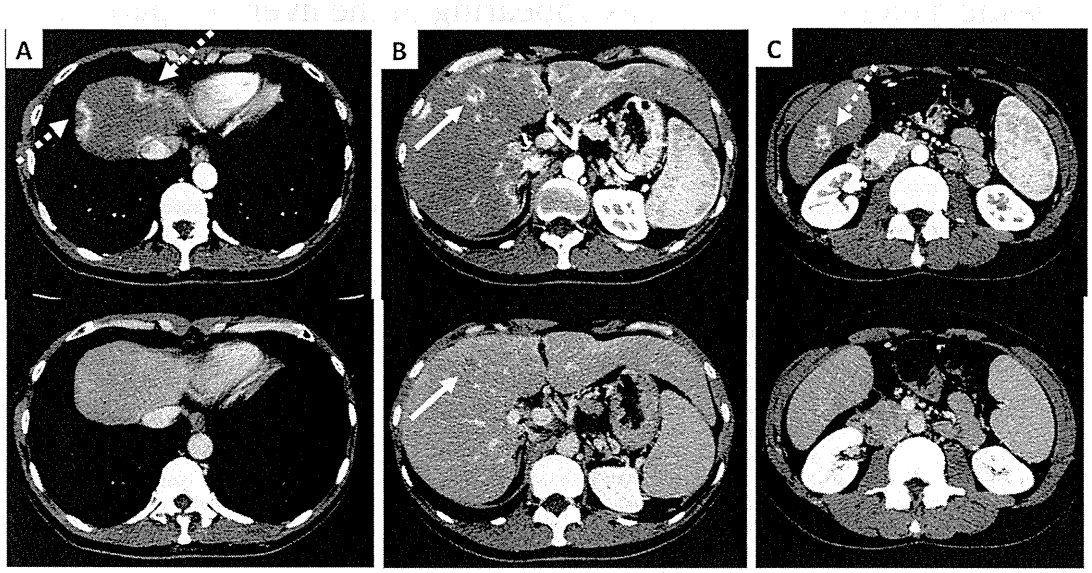

Fig. 2. Contrast-enhanced dynamic CT revealing hyperattenuation in the arterial phase and hypoattenuation in the equilibrium phase in the nodule that was finally diagnosed as cHCC-CC (Panel B, arrow). Other nonneoplastic lesions showed ring-enhancement in the arterial phase without hypoattenuation in the equilibrium phase (Panels A and C, dotted arrow). In each panel, upper image is arterial phase, and lower image is equilibrium phase.

lesions, and the internal echo showed a mosaic pattern (Fig. 1A). Contrast-enhanced dynamic computed tomography (CT) revealed hyperattenuation in the arterial phase and hypoattenuation in the equilibrium phase in the former nodule, suggesting HCC (Fig. 2B). Other lesions showed ring enhancement in the arterial phase without hypoattenuation in the equilibrium phase. Ten or more such lesions were detected. Some of them, which were located near the surface of the liver, presented geographical configuration

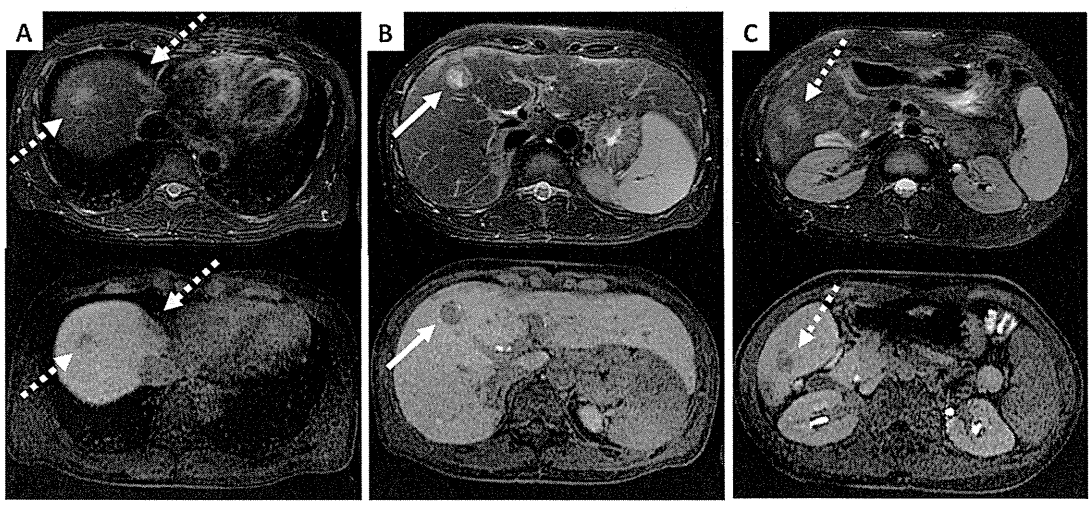

Fig. 3. Gd-EOB-DTPA-enhanced MRI revealing distinct defect in hepatobiliary phase in the nodule of cHCC-CC (down image in Panel B, arrow) and indistinct defect in nonneoplastic lesions (down images in Panels A and C, dotted arrow). In T2-weighted pre-enhancement images, the former nodule showed distinct high intensity (upper image in Panel B, arrow) and the latter showed indistinct slightly high intensity (upper images in Panels A and C, dotted arrow).